SIEMENS

The Siemens Traveling-Wave Tube RW 21

A modern power amplifier tube for Educational TV and FM microwave radio systems operating in the frequency band 2.4 to 2.8 GHz

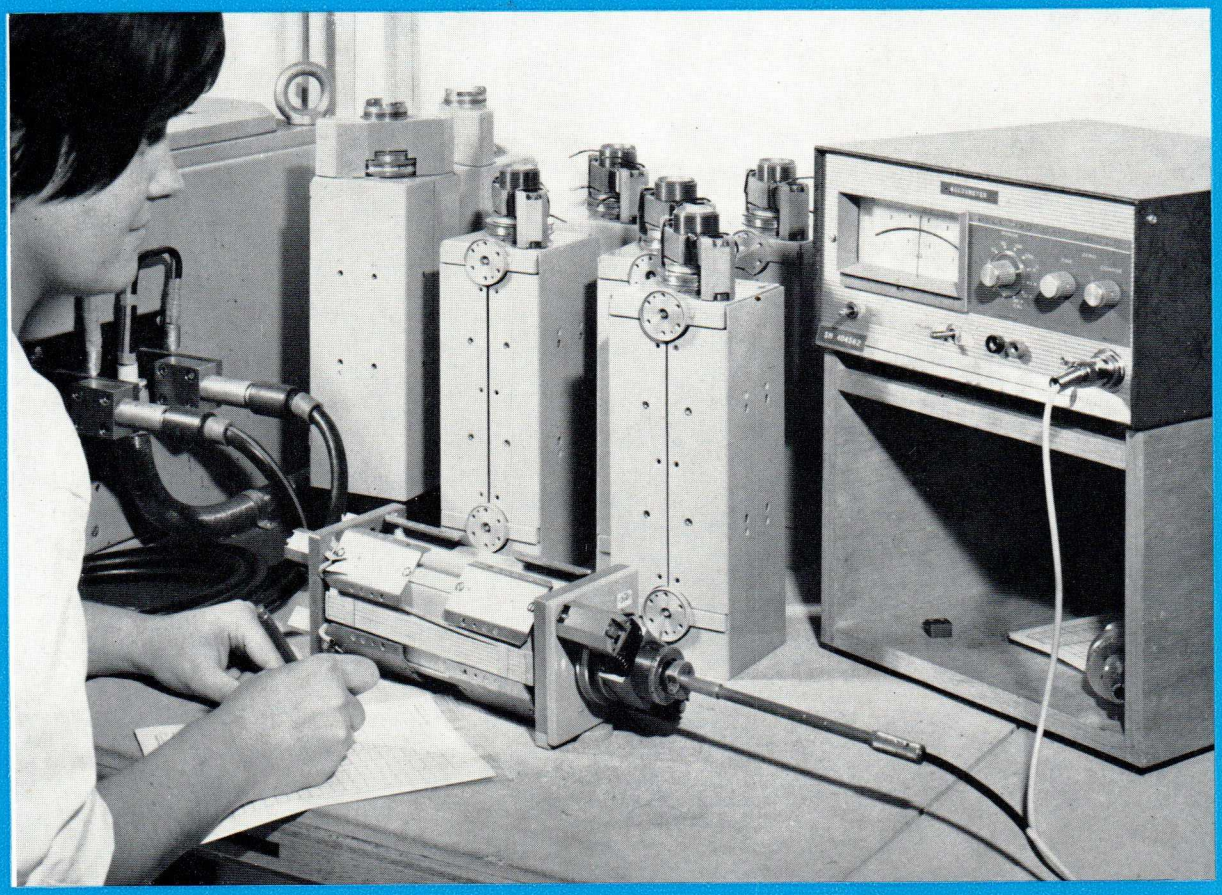

Werk für Röhren
8000 München 8, St.-Martin-Straße 76

Contents

The Siemens Traveling-Wave Tube RW 21

A modern power amplifier tube for Educational TV and FM microwave radio systems operating in the frequency band 2.4 to 2.8 GHz.

1. Introduction

The traveling-wave tube described in this article covers the frequency band 2.4 to 2.8 GHz. In ETV microwave radio equipment the RW 21 supplies a peak sync power of 10 W with common video and audio transmission at an average gain of 40 db. When employed in FM microwave radio systems output powers up to 20 W can be obtained. The pulsed saturation power is 35 W. The tube is field-replaceable as a plug-in match in its periodic permanent magnet system, requiring no readjustment of rf matching at the input or output. The compact, lightweight magnet system has a low stray field and is virtually insensitive to temperature changes. The rf input and output ports are designed for connection to coaxial circuits.

The tube is operated with depressed collector, resulting in good efficiency and low collector temperature. The AM/PM conversion at 10 W output power is 2.5 °/db. A noise figure of only 21 db is remarkably low for a tube of this power class.

2. Construction of the RW 21

Fig. 1 shows the basic construction of the RW 21. The discs (1) and (2) support the electrode system, and their outer edges ensure precise centering of the tube envelope in the magnetic focusing field. They also form part of the high-frequency circuits at the tube input and output. These discs are manufactured from a magnetic material and also serve as magnetic field shapers. The input and output antennas (3) and (4) couple the high-frequency in and out of the tube. The helix is positioned by three quarz rods [1]. The high-frequency attenuation of the helix system between output and input is about 80 db or more.

At the input end, the cathode side of the disc (1) carries a magnetic electron gun screen (8) which is inserted into the connecting tube (7). The collector in fig. 1 is electrically insolated from the helix, and can therefore be depressed. Fig. 2 shows the design of the electron gun, which consists of a 3 mm diameter metal dispenser cathode, the Wehnelt cylinder g_1 and the two flat apertured electrodes g_2 and g_3. The electron beam is focused by a combination of electric and magnetic fields. A fixed voltage negative with respect to the cathode is applied to grid No. 1, the value of which can be obtained from the data. The beam current is determined by the value of the grid No. 2 voltage, and the accelerator electrode, grid No. 3 is at helix potential, thus requiring no additional voltage supply.

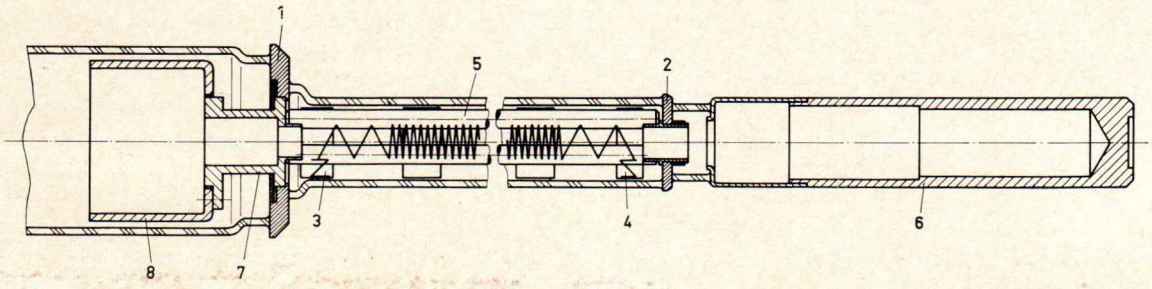

Fig. 1 Construction
of the traveling-wave tube RW 21

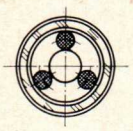

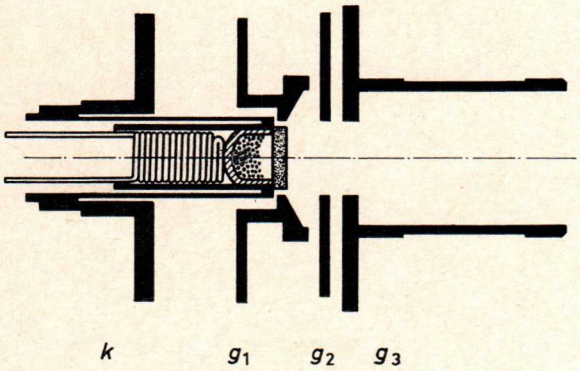

Fig. 2 Electron gun of the RW 21

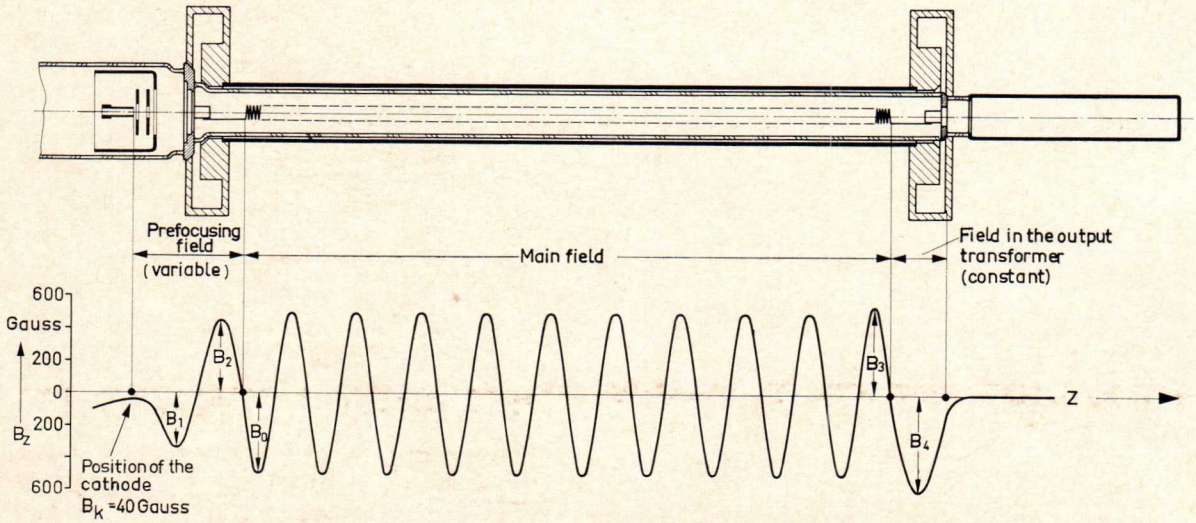

Fig. 3 Position of the RW 21 relative to the magnetic field, and axial variation of the magnetic field

3. Beam focusing and the magnet system MRW 21

The electron beam is focused by an axial magnetic field, the strength and polarity of which changes periodically. The variation of the axial magnetic field and its position relative to the tube is illustrated schematically in fig. 4. Such a periodic focusing field technique offers advantages over the more conventional permanent magnet systems in that beam stiffness is higher, the stray field considerably lower and the magnetic weight less. The sensitivity to external fields also remains lower. Details on the salient points governing the design of magnet systems for traveling-wave tubes have been covered elsewhere [2].

There are three distinct regions of the axial magnetic field: The prefocusing field with amplitudes B_1 and B_2, the main field with a peak amplitude B_0 and the field in the proximity of the output antenna with amplitudes B_3 and B_4.

Two vertical comb-like rows of pole pieces stacked one on top of the other produce the main field. Equal magnetization of the two pole piece rows is provided by the two Alnico V bar magnets.

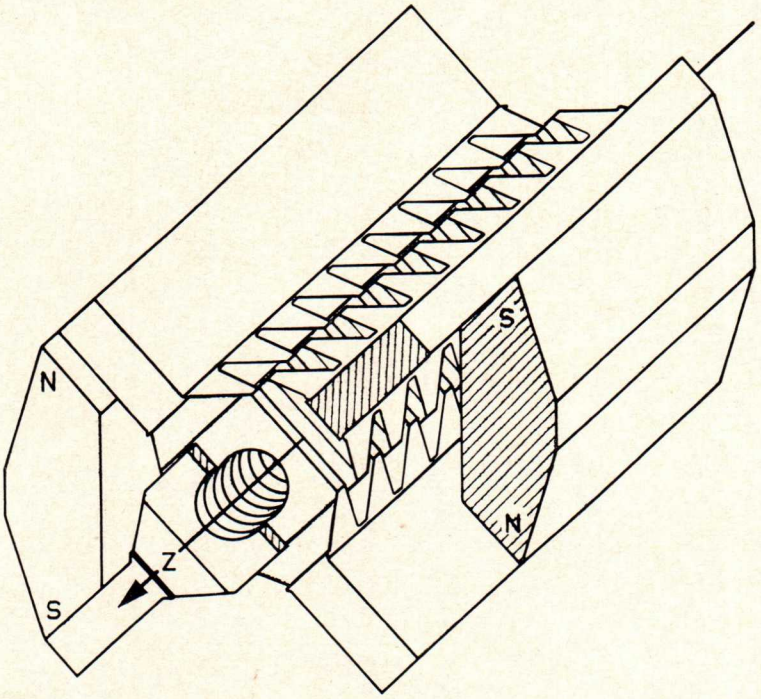

Fig. 4 Construction of the periodic permanent magnet

Magnetic fields therefore exist in the gaps between the pole pieces, the polarities of which vary periodically along the z axis. The peak magnetic field strength is approximately 500 Gauss and the period about 20 mm.

The individual field strength amplitudes are uniform, since pole pieces of like polarity are interconnected and therefore have the same magnetic potential.

The design selected and the magnetic material employed results in a magnetic focusing circuit virtually insensitive to temperature. The mechanically rugged unit is also used as a mounting base for the external coaxial circuits, the cooling and adjustable prefocusing field correction assemblies.

The magnetic field strengths B_3 and B_4 in the transverse plane near the output are somewhat higher to counteract beam divergence when the beam is modulated. The magnetic field at the collector is negligible, and the beam spreads somewhat to hit the inside of the collector diffusely.

The amplitudes B_1 and B_2 of the prefocusing field, which is coupled to the main field, can be set individually for optimum focusing. Fig. 5 shows a magnet system with a dismantled prefocusing assembly. The amplitude of B_2 is factory-preset by shifting the magnetic shunts (1) within the focusing field. The amplitude B_1, however, can be adjusted externally for minimum helix current for each tube. This is carried out with the aid of the axial field correction ring (4), which when rotated shifts the soft iron cylinder (3) axially. Two radial field correction rings (2) produce directional and polarity asymmetries in the field, and thus compensate for small variations in beam direction from tube to tube. Each ring has a soft iron segment attached to its inner surface, and both segments can be rotated in a plane normal to the axis either in opposite directions or together in one direction. The position of the segments determines the location and direction of the compensating field.

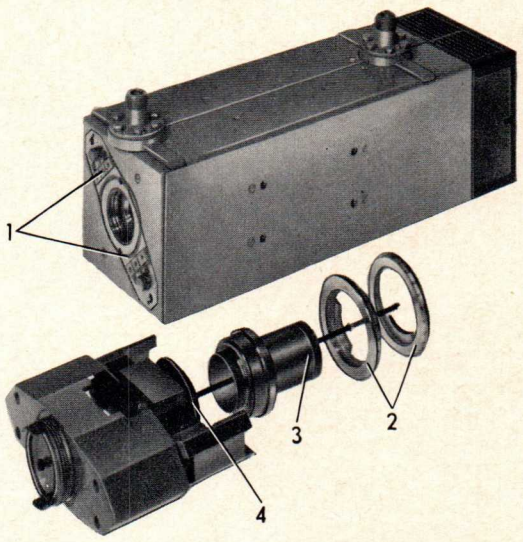

Fig. 5 Magnet system showing dismantled pre-focusing section

The axial and radial field-correction rings are set to an optimum when the helix current has been reduced to its minimum value, and to achieve this the various rings must usually be adjusted alternately several times.

A weak axial field exists at the cathode, which together with the high current density of the metal dispenser cathode favorably influences the noise properties of the tube.

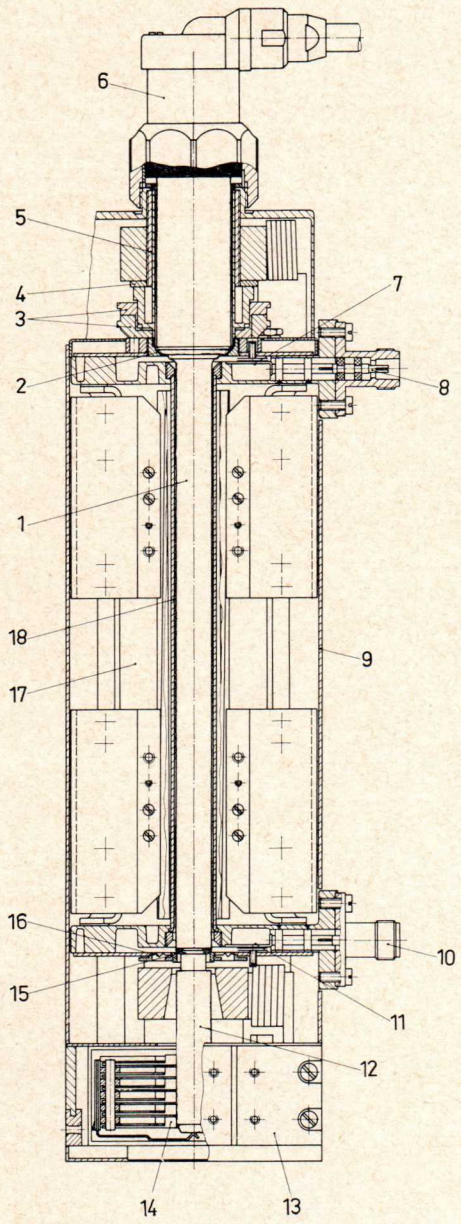

Fig. 6 Section through the magnet system MRW 21b12 with tube RW 21 and connector socket bent in direction D

1 Tube RW 21
2 Centering bush (input)
3 Adjusting rings for radial field correction
4 Adjusting ring for axial field correction
5 Soft-iron cylinder
6 Tube connector socket
7 High-frequency input coupling loop
8 Coaxial inner conductor
9 Screening plate and cover
10 High-frequency output port
11 High-frequency output coupling loop
12 Collector
13 Copper plate for mounting cooling fins
14 Internal cooling fins
15 Centering bush (output)
16 Membrane
17 Permanent magnet
18 Guiding tube

The position of the tube in its magnet system is shown in fig. 6. The two rings (see (1) and (2), fig. 1) center the tube (1) in the magnet system. The ring at the output end presses on a circular knife-edge (part 15, fig. 6), and the hemispherical surface of the ring at the input end locates precisely in a cup-shaped groove (part 2, fig. 6). The membrane (16) compensates any inevitable tolerances in length. Correct beam guidance relies upon the tube being exactly centered, and it must therefore be inserted carefully in a clean state (free from dirt and metallic particles). It is advisable to rotate the tube back and forth slightly once it has been inserted, at the same time pressing lightly on the tube base, before the screened connector socket (6) is finally screwed on.

The magnet system can be fitted with a 50 Ω N connector or 7/16 socket, or 60 Ω 3.5/9.5 or 6/16 rf sockets as required. The input power is coupled via the inner conductor (8) and antenna loop (7) into the radial resonator, and from there capacitively to the helix. The amplified signal is coupled out into the output circuit in a similar fashion.

The electrons hitting the collector lose their energy in the form of heat, which is conducted away through the cooling fins (14) to the two surfaces (13) of the cooling assembly as shown in fig. 6. The two surfaces are electrically insulated from the collector by aluminum oxide ceramic discs. Suitable cooling fins may then be mounted on the two surfaces to dissipate the heat into the surroundings (see fig. 45). Another possibility of removing the heat is by convection, as described in section 7, "Cooling". A convection-cooled magnet system with the RW 21 can be seen in fig. 7.

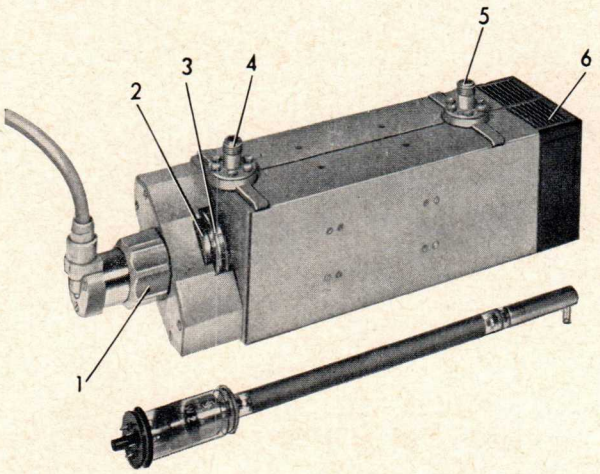

Fig. 7 Magnet system MRW 21 with traveling-wave tube RW 21

1 Tube base
2 Adjusting ring for axial field correction
3 Adjusting rings for radial field correction
4 Coaxial rf input port
5 Coaxial rf output port
6 Cooling assembly

4. Non-linear distortion

Non-linear distortion occurs when the output voltage of some transmission system is a non-linear function of the input voltage, whereby both the relationship between the input and output amplitudes and between the input and output phase is significant.

4.1. Influence of non-linear distortion on the amplification of a tv signal

The traveling-wave tube RW 21 is typically operated at 2.5 GHz as a power output tube in microwave radio systems for Educational TV (ETV) to amplify an amplitude-modulated video signal to a peak sync power of 10 W concurrently with a frequencymodulated audio signal.

The transmission properties applicable in this case must be evaluated differently from those applying to normal FM systems. The amplitude non-linearity in particular can impair the amplified tv signal, and it is therefore important that, for example, the luminance levels should not be shifted or the sync pulse amplitude compressed beyond the admissible limits. Furthermore, when the tube is operated at lower power levels as a common audio and video amplifier, no patterning due to intermodulation between the sound and video carriers must be visible in the picture. This assumes a sufficiently small phase change with drive level.

In color transmission with a chrominance subcarrier according to NTSC, the requirements on amplitude and phase linearity become even more stringent, since the color information is superimposed on the chrominance subcarrier in the form of simultaneous amplitude and phase modulation. The luminance signal is added to the chrominance subcarrier, which is then transmitted at all luminance levels between black and white. If the amplifier tube exhibits gain and phase characteristics dependent on the drive level, or in other words on the luminance level, these would produce spurious modulation of the chrominance subcarrier and hence hue changes depending on the luminance level.

The degree of influence and terms of non-linear distortion are covered in more detail below.

4.2. Distortion definitions

4.2.1. Summary

As the level of drive to the tube increases, the relationship between input and output voltage can change, not only in value but also in phase.

This is illustrated by fig. 8, which shows the locus diagram of the relative complex gain of the RW 21 with the output power as parameter. The operating point chosen is I_k = 85 mA, E_h = 1.8 kV and F = 2.6 GHz. The curve arrangement is such that for small-signal operation the gain is unity. It can be seen that for output powers up to 15 W only the phase changes, and beyond this point both the phase and the amplitude ratio (gain ratio) vary.

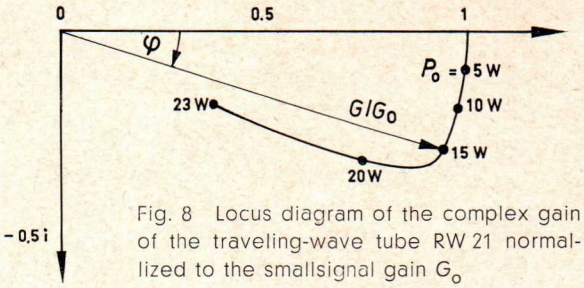

Fig. 8 Locus diagram of the complex gain of the traveling-wave tube RW 21 normalized to the smallsignal gain G_o

The negative phase angle difference means that as the drive level is increased the output phase lags behind the input phase.

Both components of the gain — gain ratio and phase — have their own significance in the evaluation of distortion.

The change of gain ratio is characterized by the compression c, and the phase change by the AM/PM conversion figure k_p.

Each change in gain, be it in the gain ratio or phase component, will produce combination frequencies due to "intermodulation" when the appropriate signals are applied to the input.

A more detailed discussion of the individual factors and their interdependence follows in the next section.

4.2.2. Component of the gain dependent on drive level

4.2.2.1. Compression, expansion

This section deals only with the amplitudes of the voltages and not with their phase relationship. Wherever the output voltage is mentioned, this infers the fundamental component only.

The ideal amplifier has an output voltage directly proportional to the input voltage. In practice however, a strictly linear relationship between these two voltages is practically non-existent. The gain characteristic generally takes the form of curve 1 in fig. 9, and with large signal amplitudes compression occurs, i.e. the gain decreases with increasing drive level. The drive level can be increased so far that the tube saturates ($\Delta e_o / \Delta e_i = 0$), in which case the output voltage no longer increases with input voltage.

The compression c is defined as:

$$c = (1 - \frac{g}{G}) \text{ or} \qquad (1)$$

$$c = (1 - \frac{\Delta e_o \; e_i}{\Delta e_i \; e_o}) \qquad (2)$$

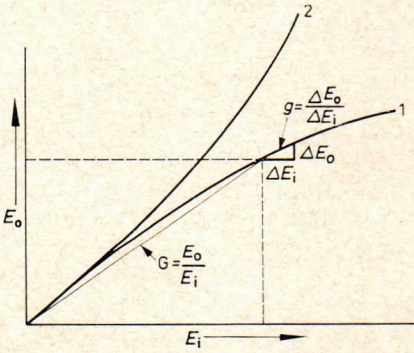

Fig. 9 Typical drive characteristics for compression (curve 1) and expansion (curve 2)

where G is the gain for the input voltage e_i and g is the differential quotient $\Delta e_o/\Delta e_i$ at the point e_i. These values are indicated in fig. 9.

Using the expression $\Delta P/P = 2\Delta e/e$, the compression can also be written

$$c = (1 - \frac{\Delta P_o}{\Delta P_i} \frac{P_i}{P_o}) \qquad (3)$$

Usually the compression is expressed as a percentage, so the above equations must be multiplied by 100.

Example: A 10% variation in input voltage produces an 8% change in output voltage. This corresponds to a compression c of 20%. The corresponding power variations are higher by a factor of about 2, or 20% and 16% respectively.

The compression normally increases linearly with input power, i.e. with the square of the input voltage. A stair-case modulated input signal with constant step amplitude (fig. 10a) is distorted at the output as shown in fig. 10b. The ordinates of fig. 10a and 10b have been chosen such that the amplitude of the lowest step is the same in each case. This example illustrates a compression of 50% for the maximum value of the output voltage.

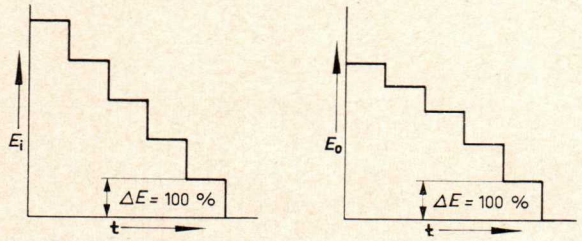

Fig. 10 Stair-case modulation waveform
a) undistorted (input)
b) distorted by compression (output)

Occasionally the relationship between output and input voltage follows curve 2 in fig. 9. This represents expansion, and the compression c has a negative value.

4.2.2.2. Pulse compression

The regions of higher output power are most affected by compression. In tv signals with negative modulation these are the sync pulses, and here the so-called pulse compression occurs. Its definition can be explained with the aid of fig. 11. If the relative pulse height at the input is S_1 and at the output S_2, then the pulse compression c_p is given by

$$c_p = \frac{S_1 - S_2}{S_1} \qquad (4)$$

This is not identical with the compression c, but represents a compression of the pulse amplitude.

4.2.2.3. Differential gain

The term differential gain originates from video techniques, and is defined as the difference in gain of a system in decibels for a small high-frequency sinewave signal at two stated levels of a low-frequency signal on which it is superimposed. (IRE Dictionary of Terms).

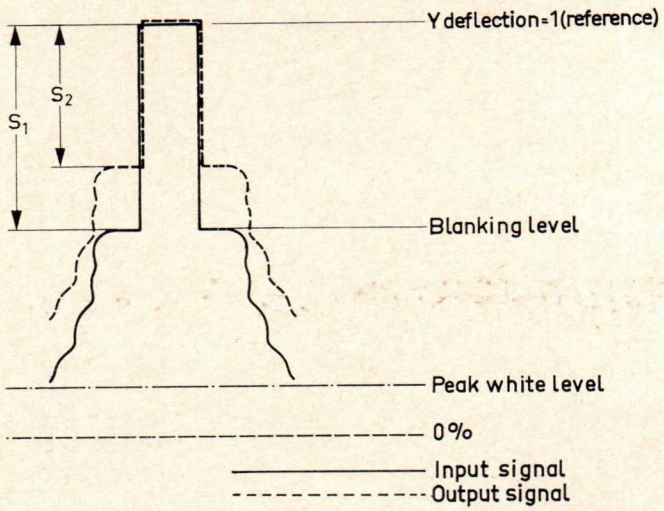

Fig. 11 Sketch to define the pulse compression

$$c_p = \frac{S_1 - S_2}{S_1}$$

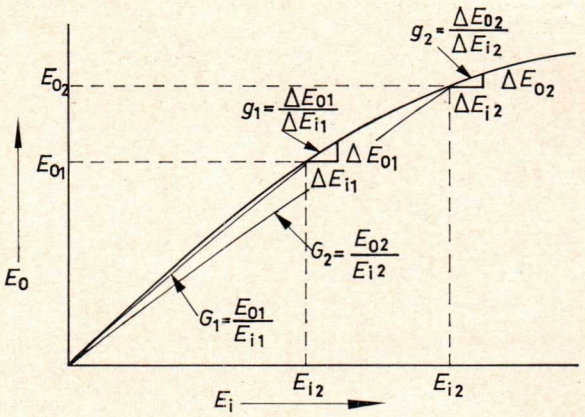

Fig. 12 Drive characteristic for defining differential gain

Since the traveling-wave tube serves as a high-frequency amplifier, it contributes only a certain portion to the total differential gain present at the video output. Experience has shown that a considerable part of the differential gain originates from the if and video stages. The degree of influence of the microwave amplifier alone can however be estimated.

If the two indices 1 and 2 (see fig. 12) are attached to the two levels (for example peak black and peak white) at which this examination is made, then

$$g_1 = \frac{\Delta e_{o1}}{\Delta e_{i1}} \text{ and } g_2 = \frac{\Delta e_{o2}}{\Delta e_{i2}}$$

The differential gain in decibels is then

$$g_1 \text{ (db)} - g_2 \text{ (db)} \qquad (5)$$

The values of g_1 and g_2 can be obtained from the compression, equation (1), so that

$$g = (1 - c)\, G \qquad (6)$$

4.2.2.4. Linearity

Another commonly used term, similar to the differential gain, is the so-called linearity.

If g_{min} and g_{max} are the minimum and maximum differential quotients of the gain within the video modulation range, for example from peak black to peak white, then the linearity is defined as

$$\text{Linearity} = \frac{g_{min}}{g_{max}} \quad (7)$$

4.2.3. Phase shift due to the variation of drive level

4.2.3.1. Phase difference Φ

The phase difference Φ is the phase angle shift between input and output voltages when the output power is increased from a small value to the value P_o. The constant portion of the phase is therefore excluded. The angle Φ corresponds to the phase angle of the gain vector in fig. 8. By plotting Φ as a function of P_o, the curve shown in fig. 13 will be obtained, using the same operating point specified in fig. 8.

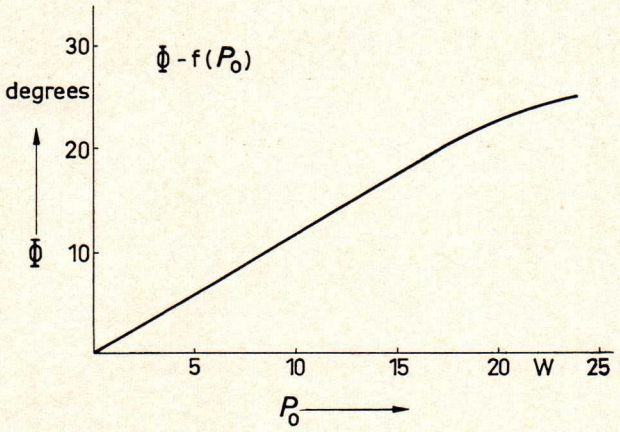

Fig. 13 Typical variation of the phase difference Φ with output power P_o

In the traveling-wave tube, the phase difference Φ generally increases linearly with the input or output power as long as no noticeable saturation effects are present. This behavior could be characterized by a coefficient expressed in degrees per watt output power for example. However, the AM/PM conversion covered in the subsequent section has more significance. This is derived from the quotient $\Delta\Phi/\Delta P_i$ and measured dynamically. It has been found namely, that direct measurement of the phase angle Φ is difficult to reproduce due to the various system temperatures at different power levels.

4.2.3.2. AM/PM conversion

If the phase difference Φ between the input and output signal depends on amplitude, an amplitude-modulated signal at the input will be phase-modulated in the tube and appear as such at the tube output. This is known as AM/PM conversion.

The AM/PM conversion k_p is defined as the change of phase angle in degrees between the input and output voltage per decibel variation in input power for a given average value of output power.

This factor is normally measured dynamically and the result expressed in degrees per decibel for a certain output power, whereby the input level should be changed by such a small amount that an even smaller variation has no effect on the result.

$$\text{Therefore} \quad k_p = \frac{\Delta\Phi}{\Delta P_i} \quad (8)$$

where ΔP_i is the incremental change in input power level in db and $\Delta\Phi$ the associated change in phase shift in the tube.

$$\text{Since} \quad p_i = 10 \log \frac{P_i}{P_o}$$

$$\text{if } P_o = 1 \text{ mW}$$

$$\text{then } \Delta p_i = \frac{10}{2.3} \frac{\Delta P_i}{P_i}$$

$$\text{and } k_p = 0.23 \frac{\Delta\Phi}{\frac{\Delta P_i}{P_i}} \quad (9)$$

Since the AM/PM conversion k_p varies with drive, the actual k_p value must be quoted in conjunction with a particular power output.

In those regions where the phase difference Φ is proportional to the input voltage, Φ can be expressed in terms of k_p as follows:

$$\Phi = 4.34\, k_p \quad (10)$$

4.2.3.3. Differential phase

Like the differential gain, differential phase is another term with its origin in video techniques. It also refers to the modulation envelope on the high-frequency carrier signal.

The differential phase is the difference in phase shifts of a small video signal (e.g. with the chrominance subcarrier frequency) at two defined drive levels, for example at 10% and 70% modulation.

The effect of the if and video stages on total differential phase is even more pronounced than on differential gain.

The microwave section of the system, with the travelingwave tube acting as an amplifier, only contributes a small amount to the total differential phase. This can be easily visualized when it is considered that a certain phase shift of the high-frequency signal caused by a change in drive level is associated with a lower phase shift of the envelope and thus the modulating video signal in the ratio similar to that of modulating frequency to carrier frequency. At a carrier frequency of 2.6 GHz and k_p values of a few degrees per db the high-frequency portion of the differential phase remains well below one degree.

4.2.4. Intermodulation

4.2.4.1. Intermodulation terms

If the relation between the amplitudes of the input and output or alternating voltage of an amplifier is non-linear, the output frequency spectrum will contain frequencies not present in the input spectrum. It is sufficient if only the phase changes and the value of gain remains constant.

The process of active components producing new frequencies from two or more original frequencies is designated intermodulation. Linear combinations from the original frequencies allow the new frequencies to be estimated or calculated.

The spurious third order products are of particular significance, the frequencies of which are

$F_{sp} = 2F_1 - F_2$ or $F_{sp} = F_1 + F_2 - F_3$.

If the original frequencies, F_1, F_2 and F_3 are close together, the spurious frequencies will also arise near the original frequencies.

In evaluating the affects of intermodulation in tv transmission, qualitatively the test picture suffices, but for quantitative results spectral analysis methods are far more suited.

4.2.4.2. Measuring procedures

a) Two tone method

Two equal-amplitude test frequencies F_1 and F_2 within the frequency band as shown in fig. 14 are used. If non-linearities exist in the amplifier intermodulation products occur at the output, those at frequencies $2F_1 - F_2$ and $2F_2 - F_1$ being of particular interest. With gain independent of frequency, the two "sidebands" will have the same amplitude. The difference in level in decibels between the side band and carrier amplitudes is employed as a measure for the magnitude of the non-linearity and designated the "two tone intermodulation ratio" IM_2 referred to a certain output power. In tv transmission the reference level for the output power is the peak of the envelope modulation (peak sync) which is 6 db above the carrier amplitude.

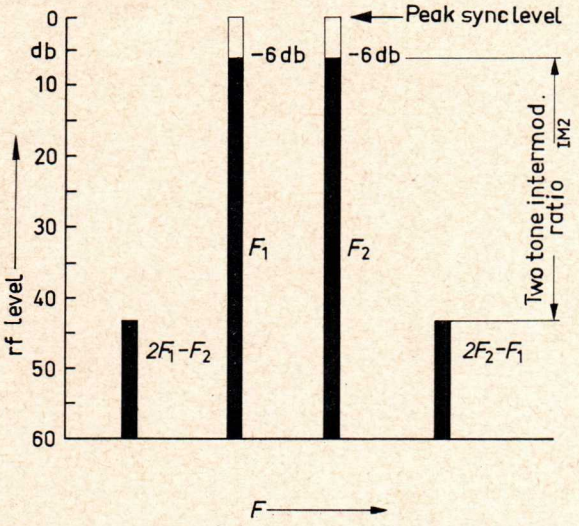

Fig. 14 Spectrum with levels for the two tone method

b) Three tone method

Although the three tone method requires more extensive measuring facilities than the two tone, it does resemble the conditions of transmission with a tv signal more closely, in particular the ratio of the average power to peak power. The two tone method produces too high a value of average power. The high frequency tv signal is simulated by the video carrier F_v, upper sideband F_{sb} and audio carrier F_a as shown in fig. 15. The frequency spacing between video carrier and sideband can be varied.

Intermodulation produces spurious frequencies within the channel, the largest an amplitude being at the frequency $F_{sp} = F_v + F_a - F_{sb}$. The various levels are shown in fig. 15. The reference level, peak sync, corresponds to the amplitude of the video carrier over the duration of the sync pulse, and the amplitude of the audio carrier is 7 db less, corresponding to the 5:1 difference between video and audio output power valid in Europe. The amplitude of the video carrier is such that in conjunction with the sideband amplitude full black to white modulation occurs. It has been assumed here that the video carrier is reduced by 6 db in the receiver due to the Nyquist flank, but not the upper sideband.

The degree of intermodulation is indicated by the difference in level in db between the sideband (F_{sb}) and the spurious product (F_{sp}) designated here and in the data, section 5.1, three tone intermodulation ratio IM_3.

4.2.4.3. Relationship between intermodulation ratios IM_2 and IM_3

The relationship between the two values can only be expressed approximately, since, as mentioned above, the average value of output power differs with the two test methods. If this difference is neglected, and the same peak powers assumed in both cases, then for a 7 db difference in level between the video and audio carriers (European Standard)

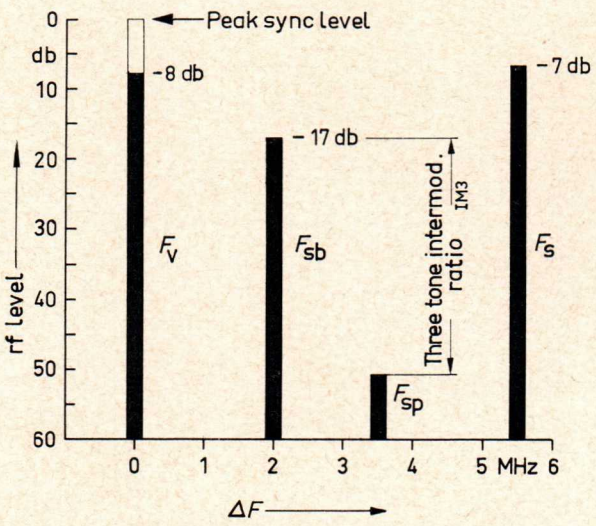

Fig. 15 Spectrum with levels for the three tone method

$IM_3 = IM_2 - 3$ db (11)

For a video to audio carrier spacing of 10 db, the values of IM_3 and IM_2 are equal. To measure this directly the level schematic detailed above must be changed such that the amplitude of the audio carrier is set to −10 db.

Under idealized assumptions (third order characteristic with constant coefficients) the following

relationship exists between the compression c, AM/PM conversion k_p and two tone intermodulation ratio IM_2:

$$IM_2 = -20 \log \sqrt{(0.125\,c)^2 + (0.019\,k_p)^2} \qquad (12)$$

4.2.4.4. Relationship to the black-to-white transition of a standard tv picture

In order to evaluate the effect of the intermodulation products on picture quality, the relationship between the intermodulation ratio, or the level of the spurious modulation, and the black-to-white transition of the tv signal. This can be explained with the aid of the three tone spectrum.

The three tone intermodulation ratio is equal to the ration of the peak-to-peak spurious modulation on the luminance signal to the black-to-white transition, if the difference in video and audio carrier amplitudes corresponds to the standard used in fig. 15.

The video carrier (amplitude about 40%, or −8 db below peak sync) is modulated to a depth of about 70% by the sideband 3 db in level below it (the video carrier is attenuated in the receiver by the operating point on the Nyquist flank). The amplitude of the video carrier is thus varied approximately between the black and white levels, i.e. between about 10% and 70% of the peak sync amplitude.

The level of the intermodulation product below the sideband amplitude thus corresponds to the level of the spurious modulation on the luminance signal below the black-to-white transition.

4.3. Linearity data on the traveling-wave tube RW 21

The main application of the RW 21 is the transmission of amplitude modulated signals, for example in Educational TV systems, and in such an application two linearity requirements are particularly important.

1. Constant gain (amplitude linearity) within a wide range of drive level.
2. Low intermodulation.

The gain as a function of output power at various characteristic helix voltages is shown in fig. 16. Various operating points can be selected depending on the characteristic which must be optimum. As can be seen, the amplitude linearity may be improved by increasing the helix voltage, but only at the expense of gain.

The following figures stated are typical values:

Curve 1 $E_h = 1.725$ kV

This represents the optimum helix voltage for maximum small-signal gain. The maximum power output obtainable is 20 W, and the highest gain 43 db.

Curve 2 $E_h = 2.05$ kV

This is the synchronous helix voltage at a nominal output power P_o of 20 W, and represents the usual operating point for FM microwave radio systems. The AM/PM conversion is relatively low.

Curve 3 $E_h = 1.85$ kV

A good compromise between gain, linearity and output power can be obtained at a helix voltage of 1.85 kV.

The maximum power output obtainable amounts to 28 W. Up to 10 W the gain remains virtually con-

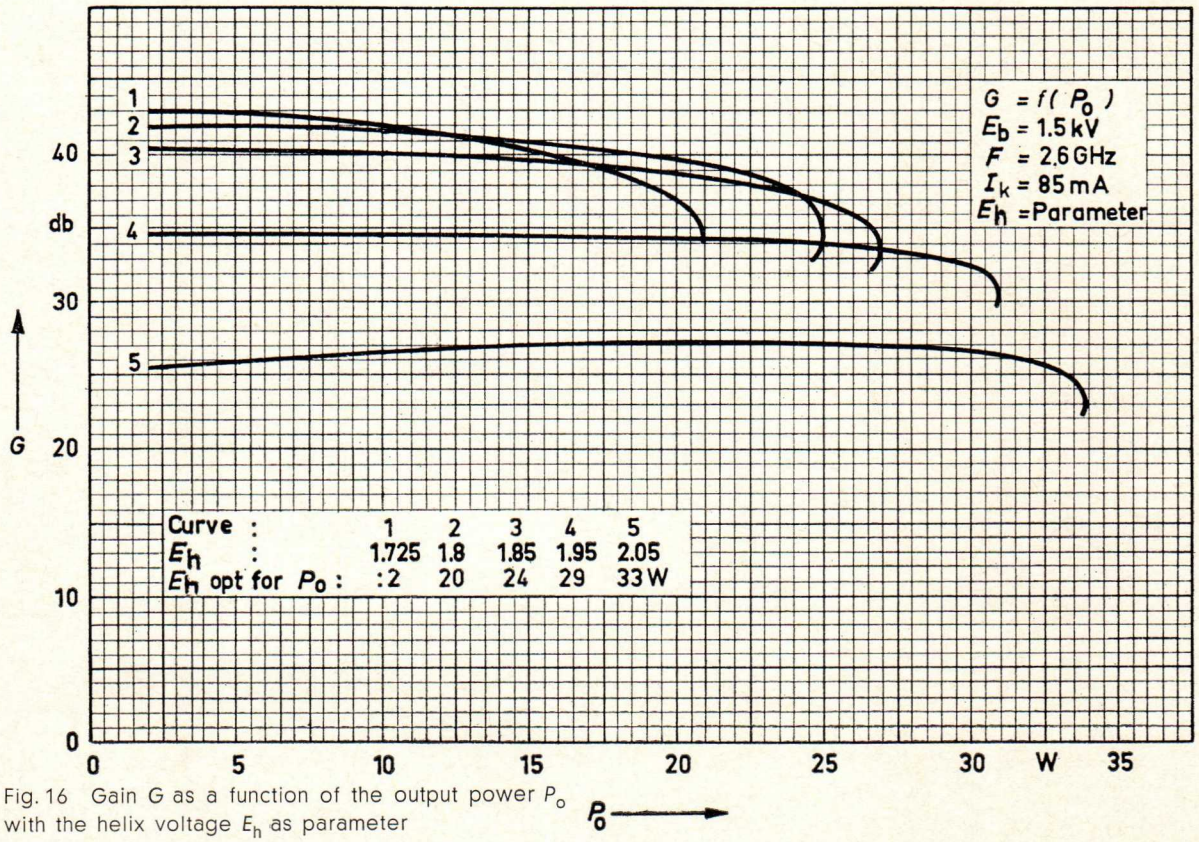

Fig. 16 Gain G as a function of the output power P_o with the helix voltage E_h as parameter

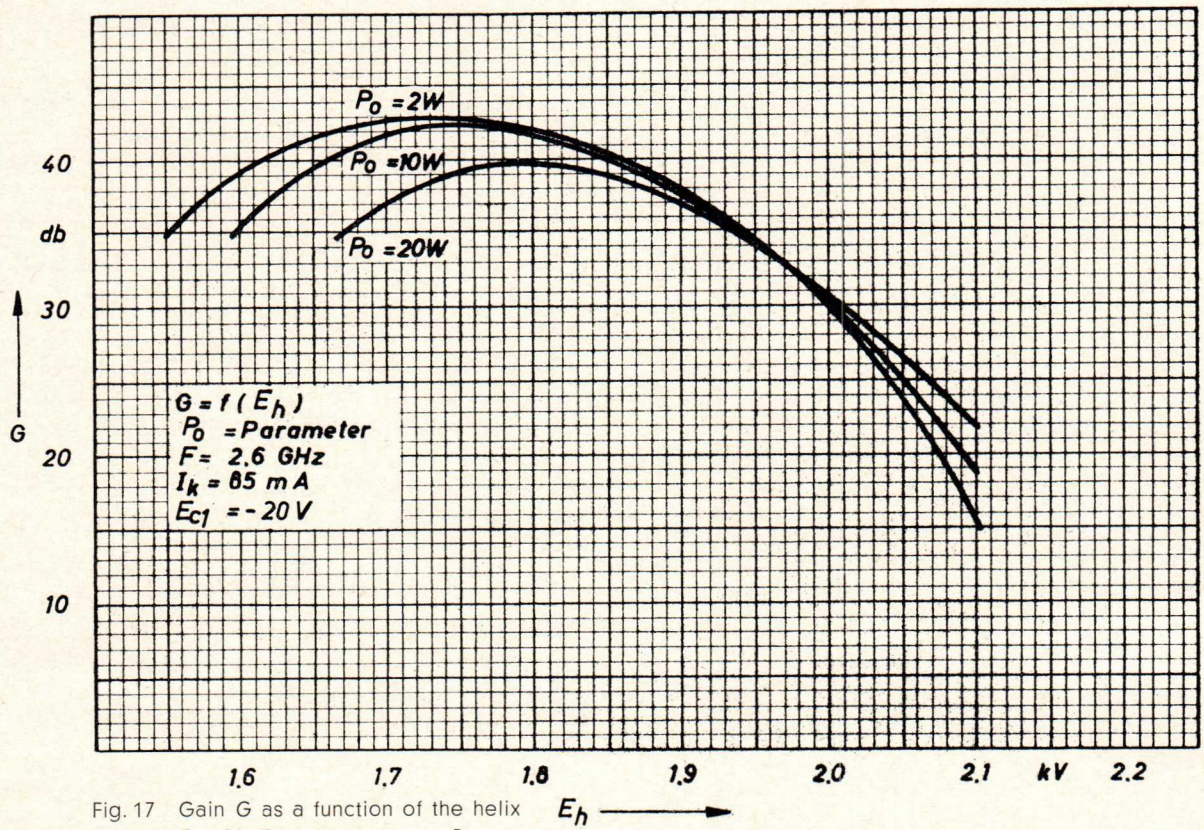

Fig. 17 Gain G as a function of the helix voltage E_h with the output power P_o as parameter

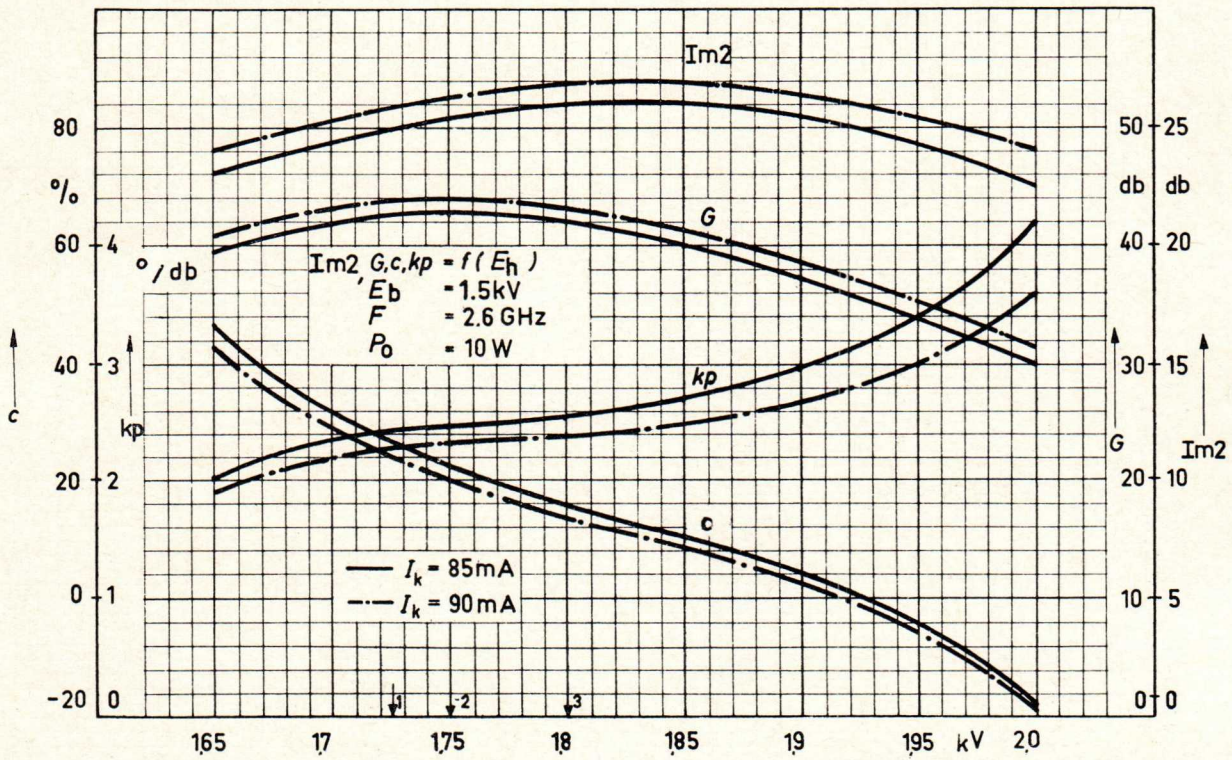

Fig. 18 Gain G, compression c, AM/PM conversion k_p and two tone intermodulation ratio IM_2 as functions of the helix voltage E_h with the cathode current I_k as parameter

1 E_h optimum for small-signal gain
2 E_h optimum for P_o 10 W
3 E_h optimum for P_o 20 W

stant, but this advantage must be compared with a gain figure about 3 db less than the small-signal gain.

Curve 4 E_h = 1.95 kV

At a helix voltage of 1.95 kV the widest linear gain range can be obtained, but the 6 db loss in gain could be considered too high. The maximum power output obtainable reaches 31 W.

Curve 5 E_h = 2.05 kV

At this helix voltage the gain lies around 27 db. The compression c is negative in the region up to 20 W, i.e. the gain increases with power.

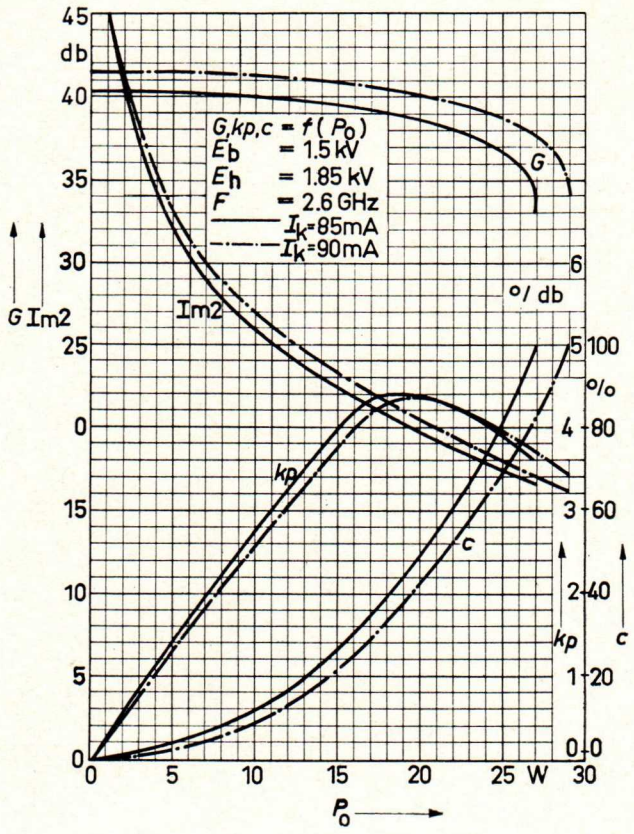

Fig. 19 Gain G, compression c, AM/PM conversion k_p and two tone intermodulation ratio IM_2 as functions of the output power P_o with the cathode current I_k as parameter

The maximum powers shown in curves 1 to 5 may only be obtained in pulse operation if they exceed 20 W, otherwise the helix could be overloaded by excessive helix current.

Fig. 17 again shows the gain, this time as a function of the helix voltage for output powers of 2.10 and 20 W.

The intermodulation conditions are illustrated by fig. 18. In addition to the gain G, compression c and AM/PM conversion k_p, the two tone intermodulation IM_2 (defined in section 4.2.4.3.) is also shown as function of the helix voltage. The usual sync level of 10 W has been chosen as output power. It can be seen that a helix voltage of 1.85 kV, corresponding to curve 3 in fig. 16, also represents a reasonable compromise with regard to intermodulation. By changing the cathode current I_k from 85 to 90 mA, the gain will increase by more than 1 db, although at 90 mA the maximum admissible collector dissipation will almost be reached.

For tv operation at 10 W sync power, it is therefore recommended to set the helix voltage about 120 to 130 V above the smallsignal synchronous value. The gain G, compression c, AM/PM conversion k_p and two tone intermodulation ratio IM_2 are shown in fig. 19 as functions of the output power at this operating point. If the output power increases by 3 db, the value of intermodulation ratio IM_2 decreases by 6 db. It should be noted that the output power stated for the intermodulation ratio IM_2 represents the peak envelope power.

5. General characteristics of the RW 21

5.1. Electrical data

Heating:			
Heater voltage	E_f	6.3	Vac [1])
Heater current, approx.	I_f	0.8	Aac
Preheating time, min.	t_k	2	min[2])

Method of heating: indirect ac, parallel supply
Cathode: metal dispenser type

Characteristics F 2.6 GHz, I_k 85 mA:

		min.	nom.	max.	
Pulsed saturation power	P_{sat}	27	35		W
Small signal gain	G	39	43		db
Gain at P_o 20 W	G	36	40		db
VSWR	s		1.35	1.85	[3])
Cold attenuation	αc		80		db
Hot attenuation	αh		80		db

Typical operating data:
I. ETV microwave radio transmitter, common video and audio amplifier, negative modulation.

Video carrier frequency	F			2.6		GHz
Peak sync power	P_{syn}	5	10	5	10	W
Gain	G	40	40	41	41	db
Cathode current	I_k	85	85	90	90	mAdc[4])

3 tone intermodulation ratio:

Video-to-audio carrier spacing 10 db	IM_3	–32	–26	–33	–27	db[5])
Video-to-audio carrier spacing 7 db	IM_3	–29	–23	–30	–24	db[5])
Pulse compression, max.	c_p	15	20	10	15	
Linearity (between 10% and 70% modulation), approx.		0.96	0.94	0.97	0.95	

Collector voltage	E_b			1.5		kVdc
Helix voltage, approx.	E_h			1.85		kVdc[6])
Grid No. 2 voltage, approx.	E_{c2}	625	625	660	660	Vdc
Grid No. 1 voltage	E_{c1}			–20		Vdc
Helix current, approx.	I_h	0.8	1.0	1.0	1.5	mAdc[7])
Grid No. 2 current, max.	I_{c2}			0.1		mAdc

1) If the maximum variation of heater voltage exceeds the absolute maximum limits of ± 2 % the operating performance and life of the tube will be impaired.

2) The preheating time of two minutes applies only to the first time the tube is fired up. If the mains voltage fails, the tube can be switched on again without preheating under the conditions detailed in section 6.2.3. "Switching on and off".

3) At the input and output of the cold tube over the frequency band 2.4 to 2.8 GHz.

4) Adjust E_{c2} to give the appropriate value.

5) This value corresponds to the difference in level between the spurious modulation on the luminance signal (peak-to-peak) and the black-to-white transition, see also section 4.2.4.4.

6) Helix voltage about 125 Vdc above the small-signal synchronous helix voltage.

7) For black level i. e. P_o about 1/2 P_{syn}

Typical operating data:

II. Broadband microwave radio systems

Operating frequency	F			2.6				GHz
Output power	P_o	20	10	5	15	10	5	W[1])
Gain, approx.	G	40	42	42	38.5	37	34	db
Cathode current	I_k	85	85	85	75	65	55	mAdc[2])
Collector voltage	E_b	1.6	1.4	1.2	1.45	1.3	1.15	kVdc[3])
Helix voltage, approx.	E_h	1.8	1.75	1.73	1.76	1.73	1.7	kVdc[4])
Grid No. 2 voltage, approx.	E_{c2}	625	625	625	575	525	470	Vdc[5])
Grid No. 1 voltage	E_{c1}	−20	−20	−20	−30	−40	−50	Vdc[3])[5])
Helix current, approx.	I_h	3.0	2.5	2.0	2.5	2.0	2.0	mAdc
Grid No. 2 current, max.	I_{c2}			0.1				mAdc
Noise figure, approx.	NF			21				db
AM/PM conversion, approx.	k_p	4	2	1	4	3	2	°/db[6])
ΔE_h /PM conversion, approx.	$\Delta\Phi/\Delta E_h$			1.5				°/Vdc[7])

Maximum ratings (absolute values)

Cold collector voltage	E_{bb}	max	1.9	kVdc
Collector voltage	E_b	max	1.8	kVdc
Collector dissipation	P_p	max	150	W
Helix voltage	E_h	max	2.2	kVdc
	E_h	min	1.6	kVdc
Helix current	I_h	max	7	mAdc[8])
Helix dissipation	P_h	max	12	W
Grid No. 2 voltage	E_{c2}	max	900	Vdc
Grid No. 2 dissipation	P_{c2}	max	0.2	W
Grid No. 1 voltage	E_{c1}	min	−100	Vdc
	E_{c1}	max	0	Vdc
Load VSWR	s	max	2	
Cathode current	I_k	max	100	mAdc
Collector temperature	T_c	max	270	°C[9])
Magnet system temperature	T_m	max	100	°C[10])
Ambient temperature	T_A	min	−20	°C
	T_A	max	55	°C[11])
Temperature of the cooling surfaces	T_{cu}	max	115	°C[12])

1) See also section 5.2.2. for operation at reduced power levels below 20 W.

2) Adjust E_{c2} to give the appropriate value.

3) Setting value.

4) The helix voltage values specified are typical values. When designing the power supply a variable range of ± 250 Vdc should be provided.

5) Other combinations of E_{c1} and E_{c2} are possible (see section 5.2.2.). When designing the power supply for E_{c2} a variable range of ± 150 Vdc should be provided.

6) The AM/PM conversion is defined in section 4.2.3.2.

7) The △E/PM conversion is defined in section 5.3.

8) The helix current may rise momentarily to 10 mAdc due to mains surges and during starting (relay trip limit 10 mAdc).

9) If the cooling system fails or the carrier signal is removed the collector temperature may rise for a maximum of three days up to 300 °C.

10) Measured at the coaxial output plug. The lacquer should be removed from the measuring point if necessary.

11) See cooling, section 7.

12) Only valid for conduction cooling.

Dimensions oft the tube and magnet system

Dimensions of the tube	see fig. 20	
Dimensions of the magnet system	see fig. 21 100 mm×130 mm×384 mm 4"×5 1/8"×15"	without tube socket
Weight of the tube	approx. 200 gm, 7 ozs net	
Weight of the magnet system	approx. 12.5 kg, 28 lbs	
Dimensions of the tube packing	170 mm×170 mm×560 mm 6 5/8"×6 5/8"×22"	
Coaxial rf connectors	50Ω, N connector 3/7 7/16 coaxial	
	60Ω, 3.5/9.5 or 6/16 coaxial	
Mounting position	optional	
Tube base	similar to continental base. The appropriate connector socket with screened leads is supplied with the magnet system either straight or with 90° bends in any one of four directions.	

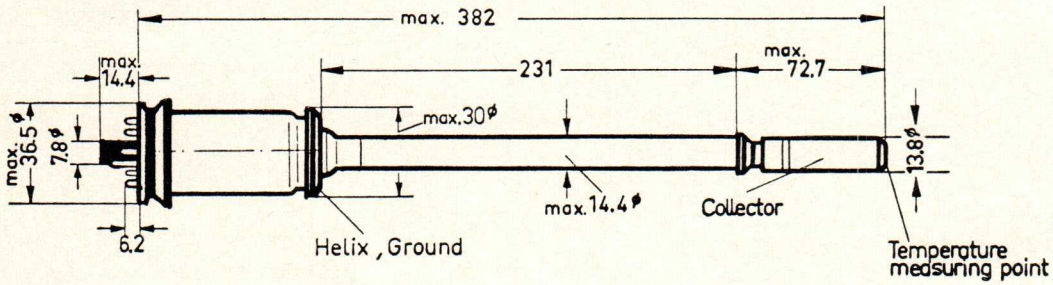

Fig. 20 Dimensions of the tube RW 21

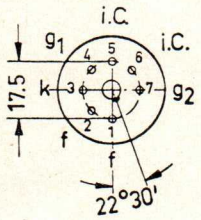

Fig. 21 Dimensions of the magnet system MRW 21

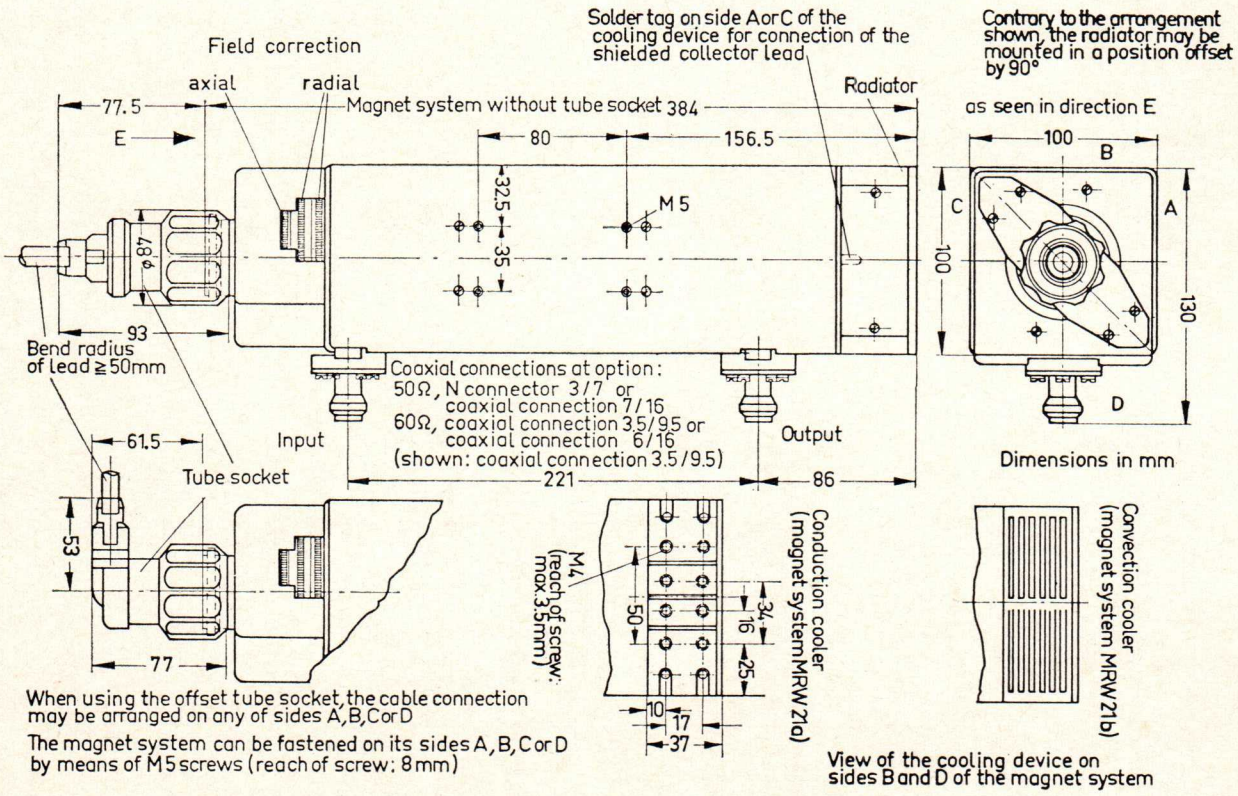

5.2. Gain and output power

At constant beam current and low input signal level, the output power is directly proportional to input power, see fig. 22. At higher levels the gain falls since the beam modulation increases, and the transfer of energy to the high-frequency field reduces the velocity of the beam electrons. In order to achieve sufficient velocity for energy transfer in spite of the velocity loss at the output, the beam velocity is increased by applying a higher helix voltage. With further increase in level of the input signal, the tube saturates, and the beam gives up the maximum possible energy. If the input power is increased beyond the saturation point, the output power falls again since the synchronous conditions are no longer fulfilled.

5.2.1. Operation at nominal output power

The graph fig. 22 illustrates the output power as a function of the input power at 2.4 GHz, 2.6 GHz and 2.8 GHz, and a direct reading of gain can be obtain-

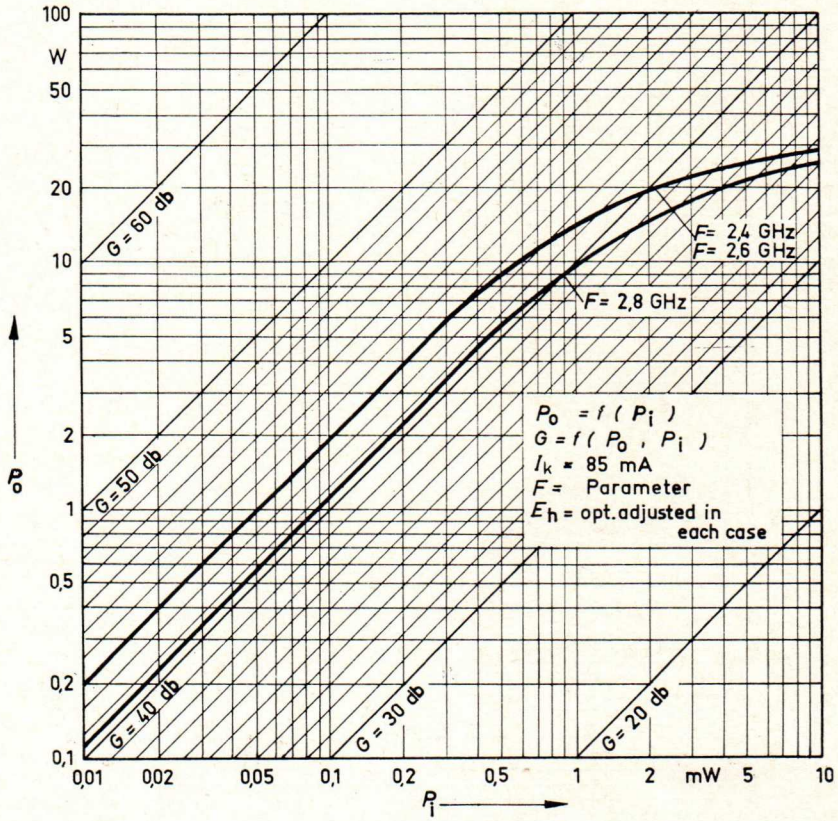

Fig. 22 Gain G as a function of the input power P_i and output power P_o with the frequency F as parameter

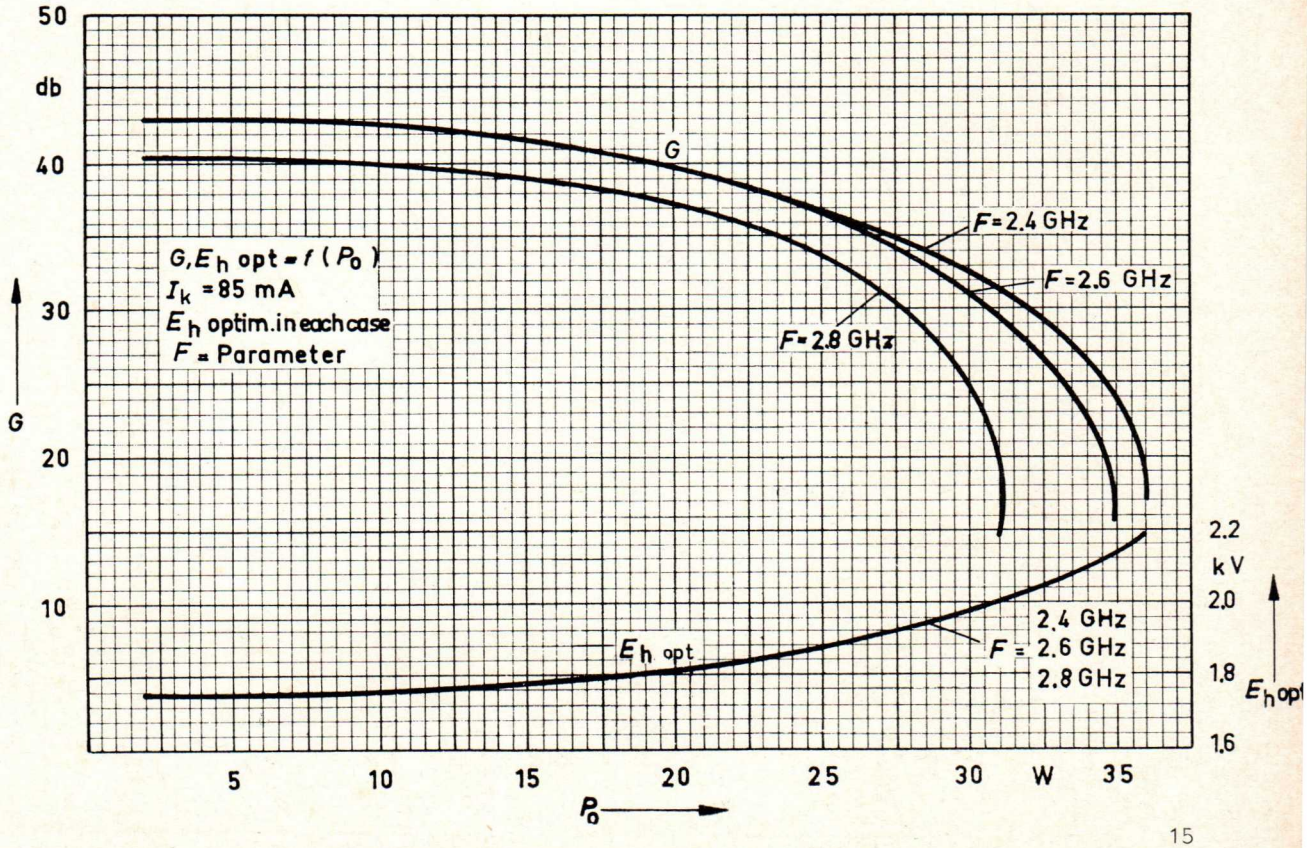

Fig. 23 Gain G and optimum helix voltage E_h opt as functions of the output power P_o with the frequency F as parameter

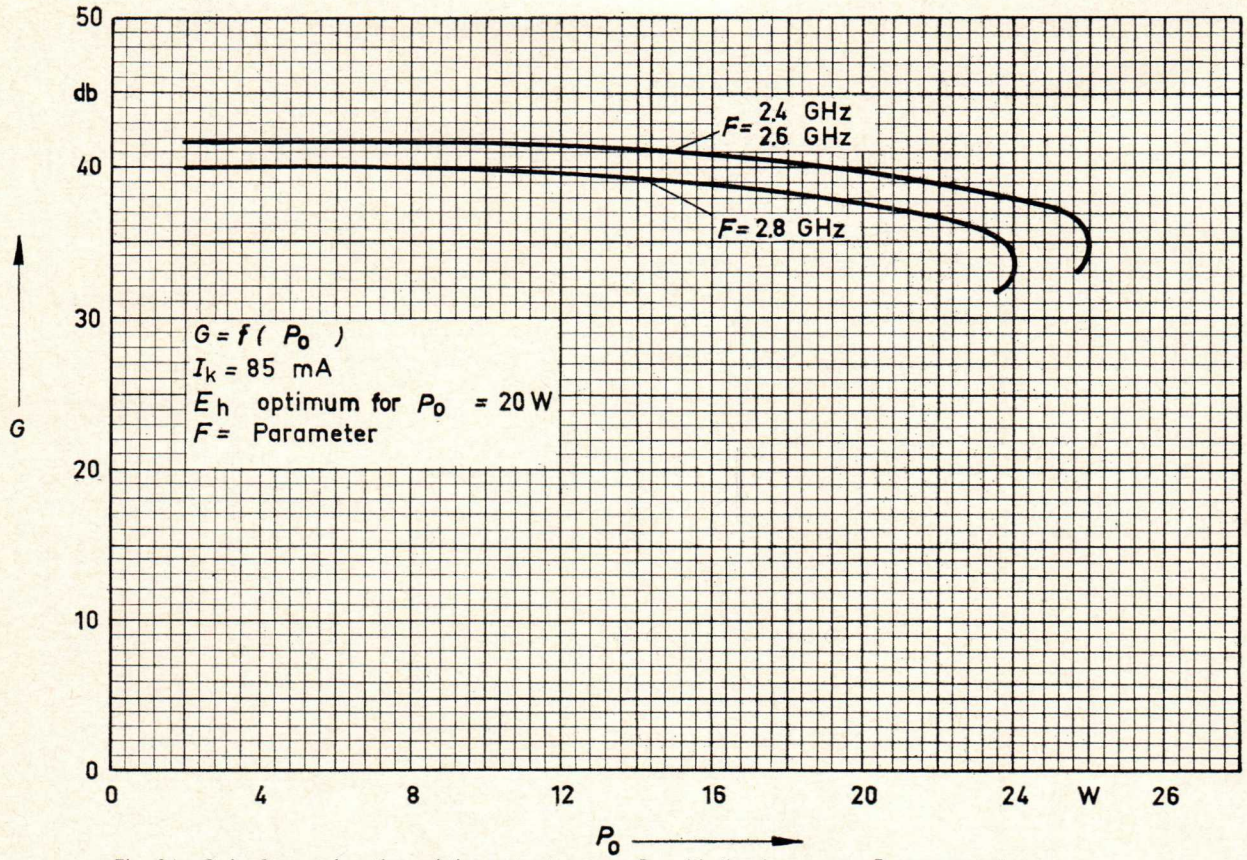

Fig. 24 Gain G as a function of the output power P_0 with the frequency F as parameter

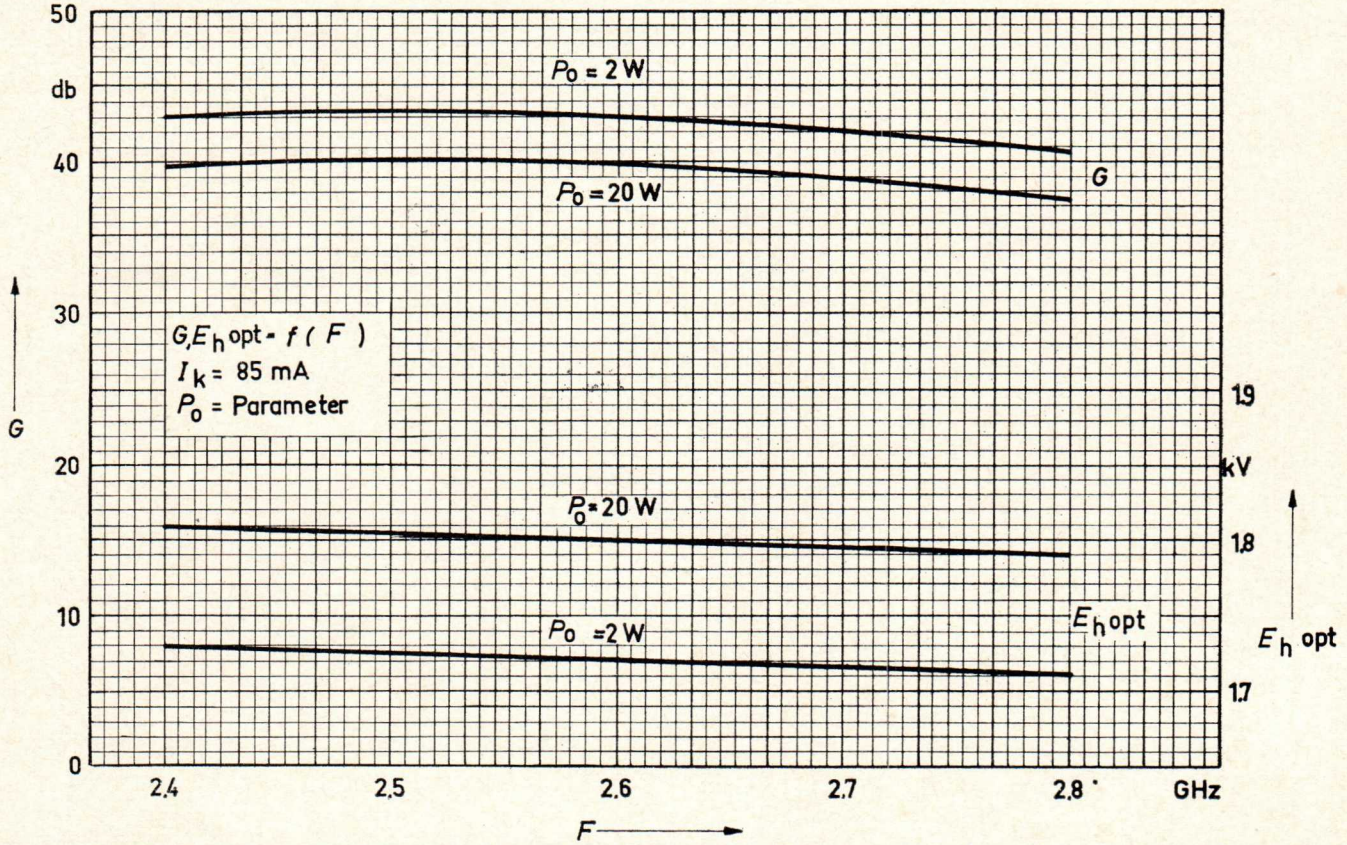

Fig. 25 Gain G and optimum helix voltage E_h opt as functions of the frequency F with the output power P_0 as parameter

ed. The helix voltage has been set for maximum gain in each case. The slightly lower gain at the upper frequency of 2.8 GHz can be explained by the fact that at higher frequencies the field lines do not penetrate into the beam so far, resulting in less interaction between the wave and beam. The larger number of wavelenghts in the tube compensates this effect somewhat and improves the final result.

Fig. 23 shows the gain and optimum helix voltage as functions of the output power; the optimum helix voltage increases with output power.

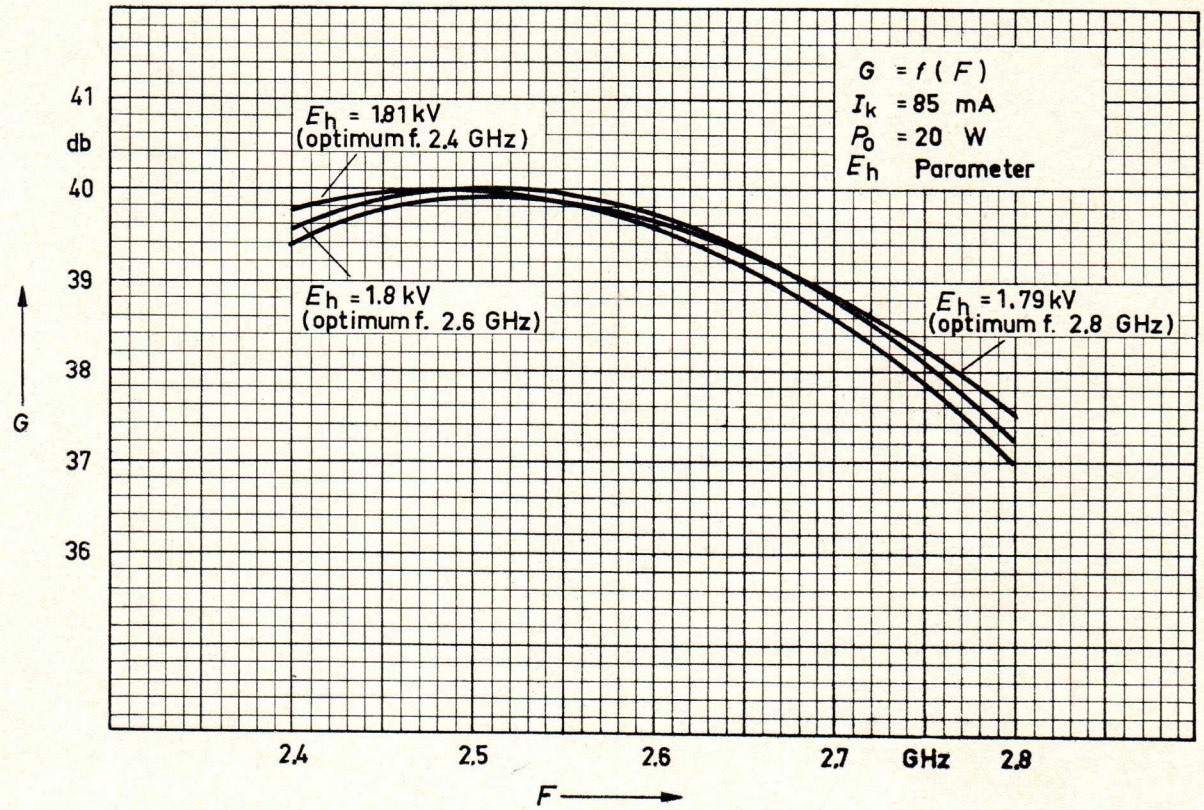

Fig. 26 Gain G as a function of the frequency F with the helix voltage E_h as parameter

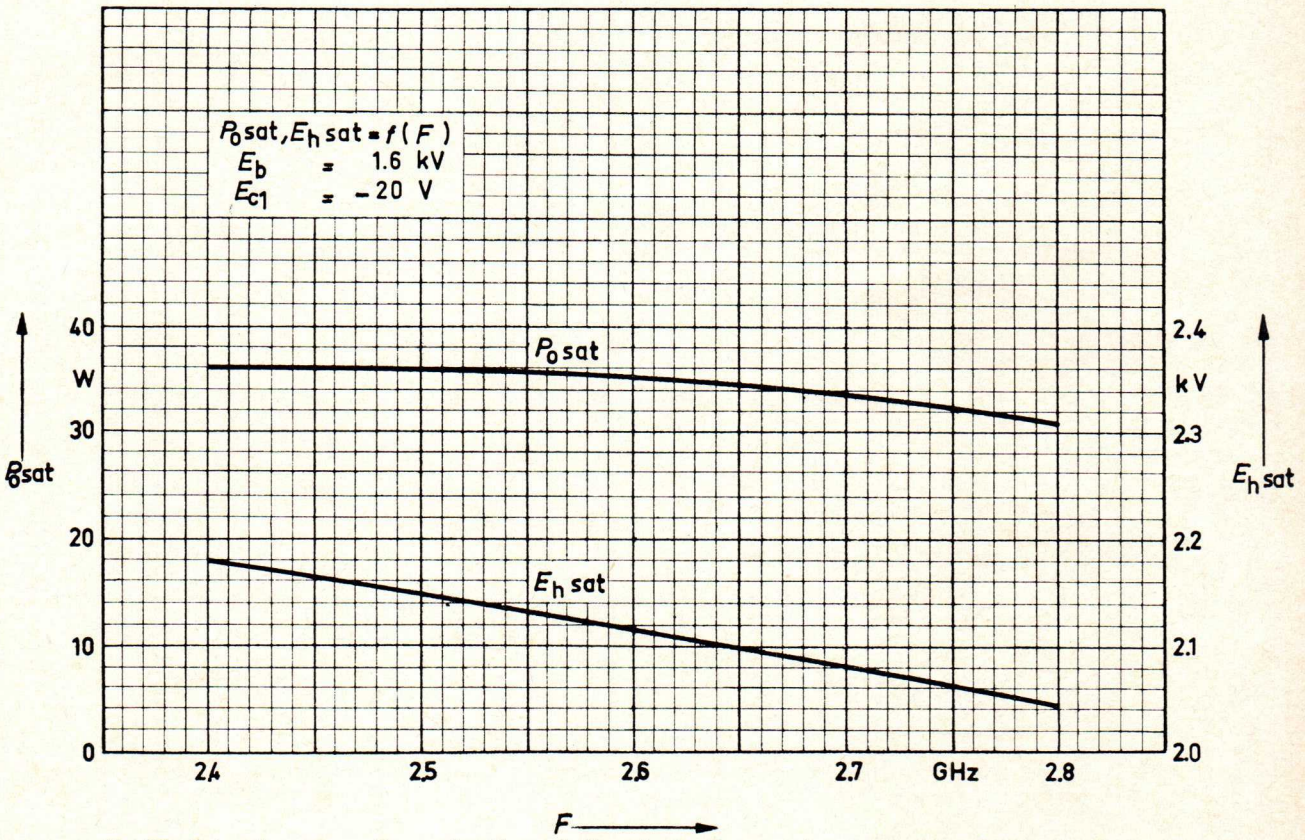

Fig. 27 Saturation power P_{sat} and optimum helix voltage $E_{h\ sat}$ as functions of the Frequency F

In fig. 24 the gain with constant helix voltage is presented as a function of the output power at three different frequencies. The helix voltage has been set to its synchronous value for an output power of 20 W.

The influence of frequency on the gain at output powers of 2 W and 20 W with the helix voltage synchronous in each case can be seen in fig. 25.

The variation of gain with frequency at 20 W output power is represented in fig. 26 for the synchronous helix voltages at 2.4 GHz, 2.6 GHz and 2.8 GHz. Fig. 27 shows the saturation power P_{sat} and associated optimum helix voltage $E_{h\,sat}$ over the frequency band 2.4 to 2.8 GHz. The saturation power de-

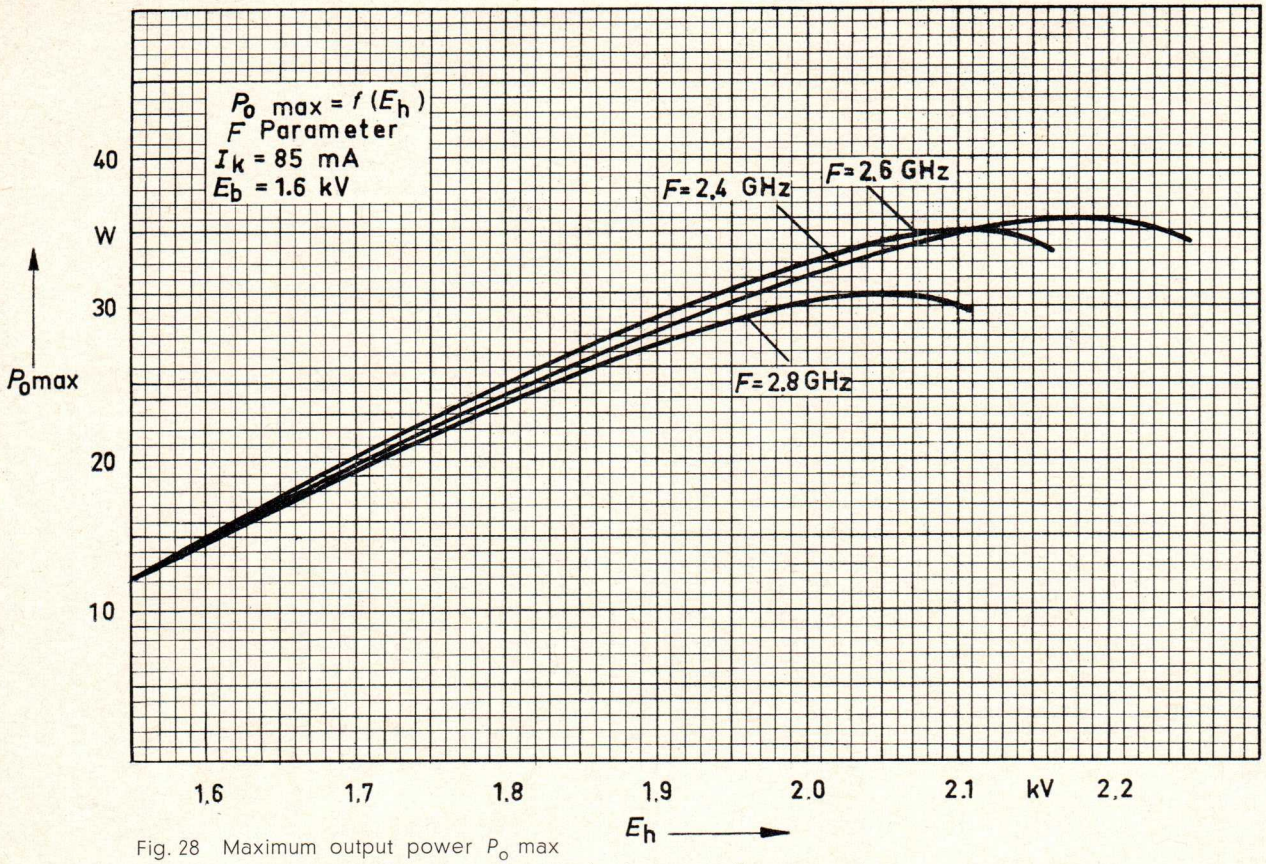

Fig. 28 Maximum output power P_o max as a function of the helix voltage E_h with the frequency F as parameter

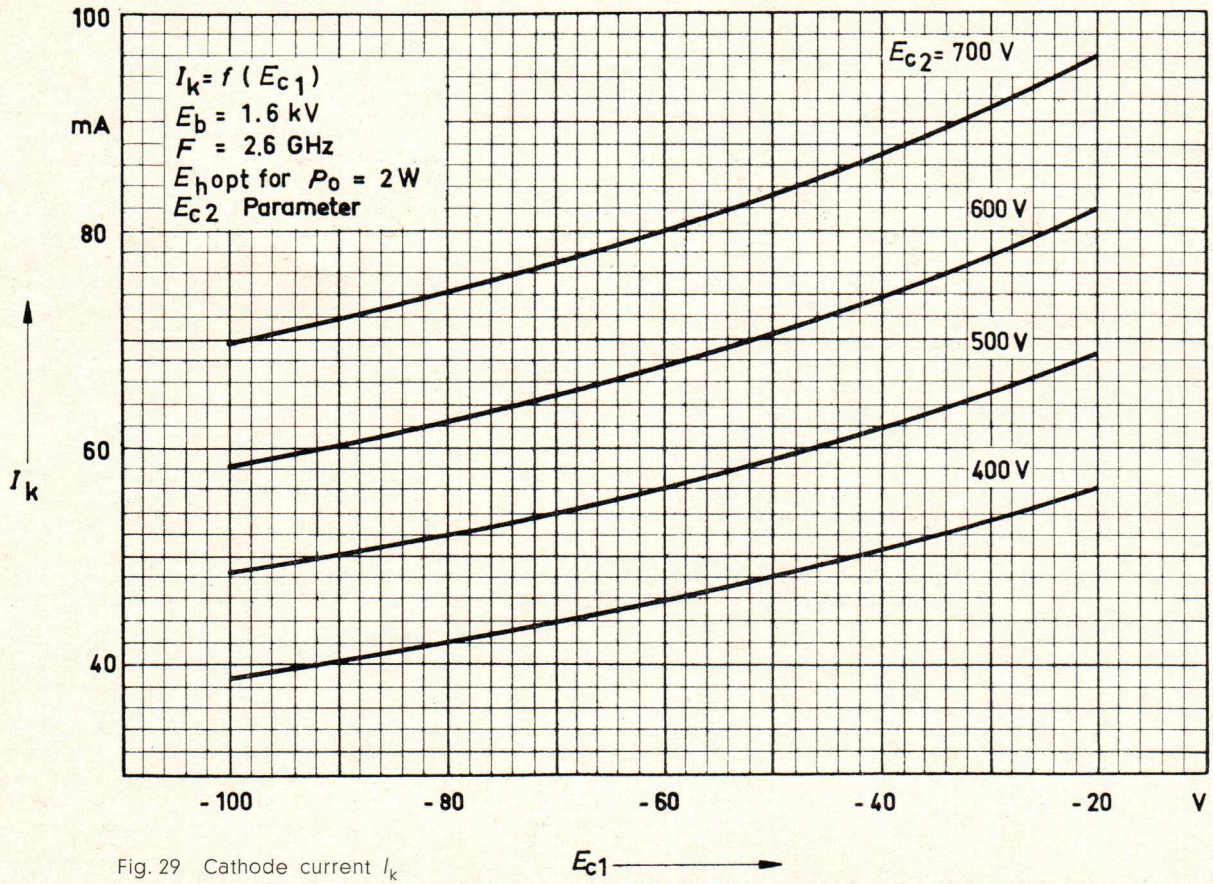

Fig. 29 Cathode current I_k as a function of the grid No. 1 voltage E_{c1} with the grid No. 2 voltage E_{c2} as parameter

creases from 36 W to 31 W as the frequency increases, and has been measured with square-wave pulses at a 1:2 duty cycle.

The value of the maximum obtainable output power P_o for three different frequencies (2.4 GHz, 2.6 GHz and 2.8 GHz) as function of the helix voltage at a cathode current I_k of 85 mA can be taken from fig. 28. The highest value of output power corresponds to the saturation power P_{sat}. If the RW 21 is operated at CW powers above 20 W,

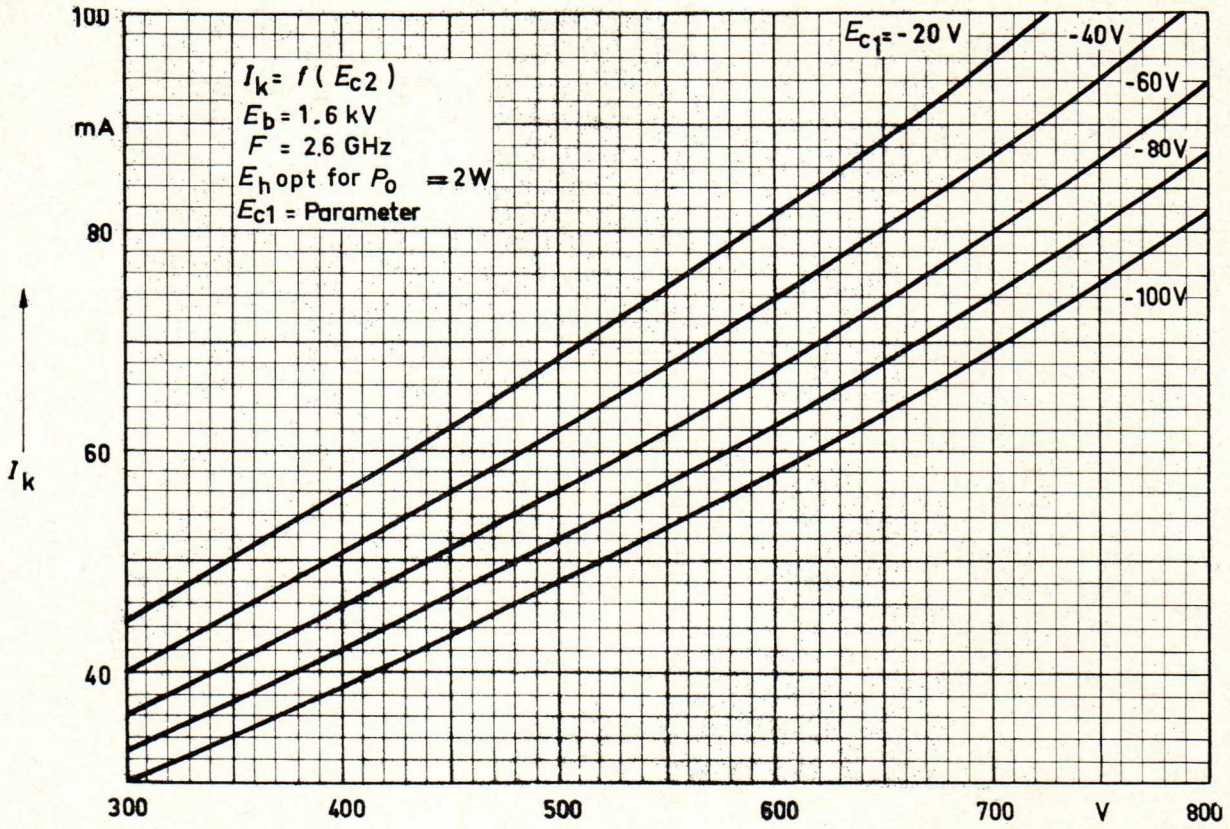

Fig. 30 Cathode current I_k as a function of the grid No. 2 voltage E_{c2} with the grid No. 1 voltage E_{c1} as parameter

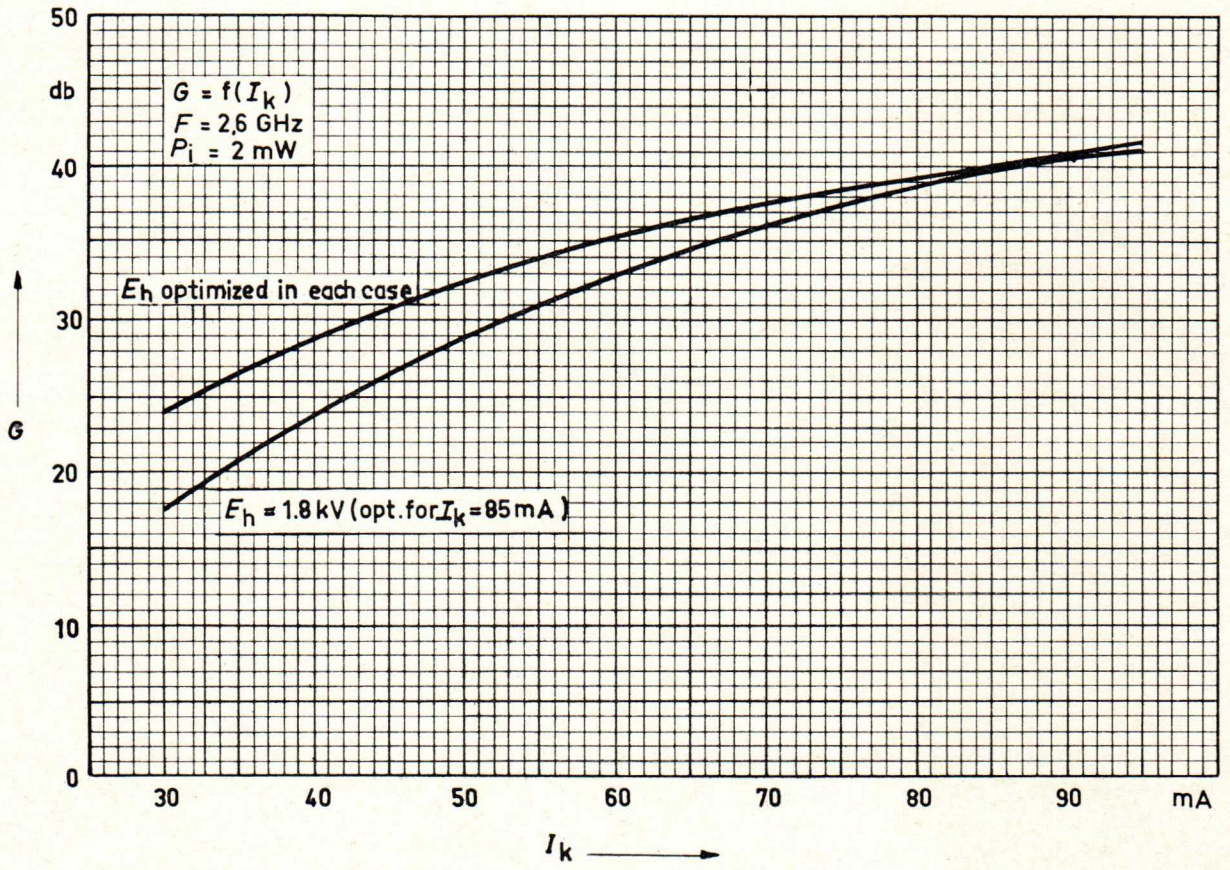

Fig. 31 Gain G as a function of the cathode current I_k

care should be taken that the maximum admissible helix current is not exceeded under any circumstances.

The influence of electrode voltage variations on the performance can be obtained from the curves in figs. 29, 30 and 31. The following values have been derived from these curves:

1. Variation of gain with cathode current

$\frac{\Delta G}{I_k}$ approx. 0.2 db/mA

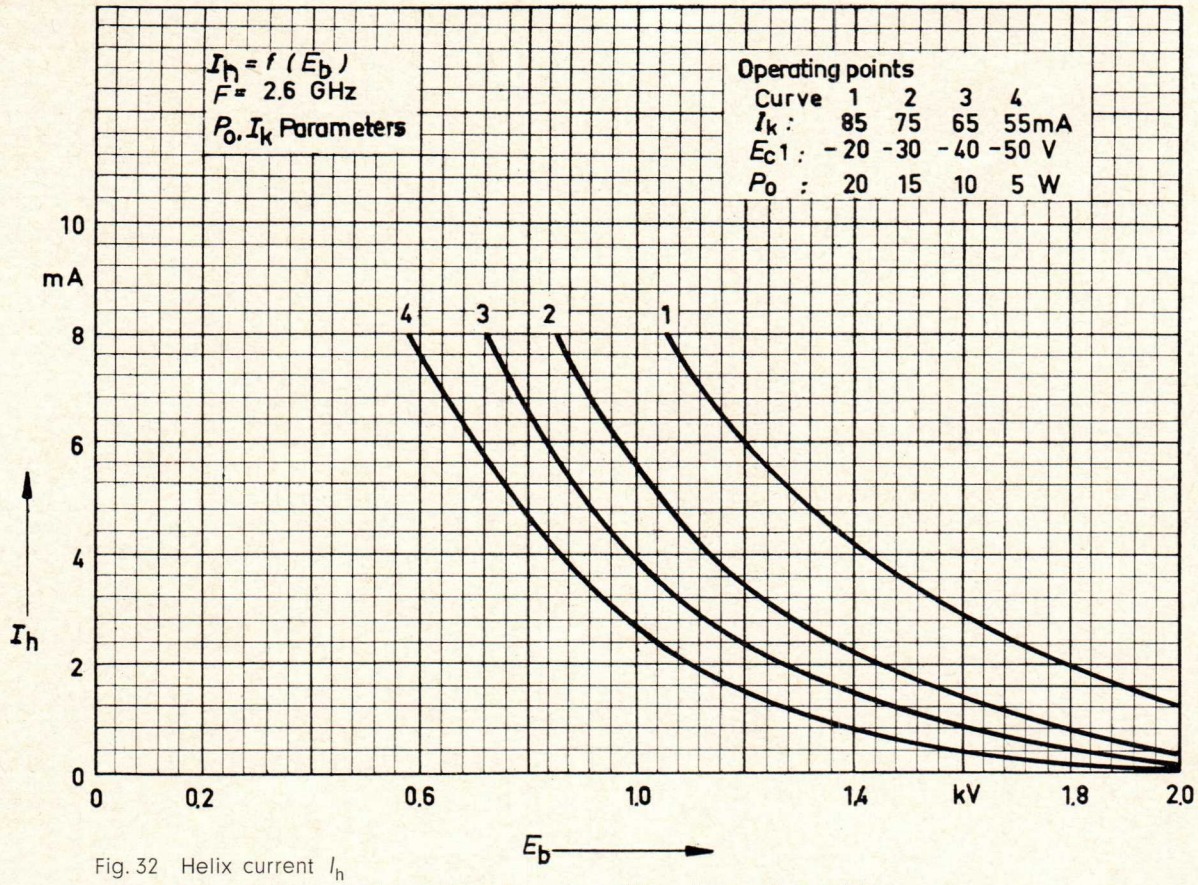

Fig. 32 Helix current I_h as a function of the collector voltage E_b at four different operating points

at the following operating point:

I_k 85 mA
P_o approx. 20 W
P_i constant
E_h constant (optimum for 20 W)

2. Transconductance of grid No. 1 and grid No. 2

$\frac{\Delta I_k}{\Delta E_{c1}}$ approx. 0.45 μmhos

with $I_k = 85$ mA and E_{c2} constant.

$\frac{\Delta I_k}{\Delta E_{c2}}$ approx. 0.15 μmhos

with $I_k = 85$ mA and E_{c1} constant.

5.2.2. Operation with reduced power

If a traveling-wave tube is operated well below its nominal output power, the operating efficiency can be improved by readjusting the electrode voltages. There are two main possibilities open:

a) If high linearity (either low AM/PM conversion or good amplitude linearity) and large gain values are required, the normal beam current should be retained. On the other hand the collector voltage can be reduced considerably, depending on the output power desired; this should not be in the region of helix current increase (see fig. 32). Fig. 33 shows the relationship between helix current I_h and collector voltage E_b for four different powers with a constant cathode current of 85 mA. If the collector voltage is too low, the slowest electrons can no longer reach the collector and return to the helix. The number of slow electrons increases with the amount of energy removed from the beam. All other electrode voltages such as E_{c1}, E_{c2} and E_h remain unchanged.

b) If a certain amount of relaxation in linearity and gain requirements can be tolerated, a further improvement in operating efficiency over a) above can be achieved, when, in addition to the collector voltage, the cathode current is reduced.

This alternative is made use of if for a given input power the output power, and thus the gain, may be lower than normal, as is the case, for example, in a microwave radio network with hops of varying length.

Operation with reduced cathode current and collector voltage when the amplifier cooling system fails can also be quite a useful feature. If the tube is operated under normal conditions without cooling (see section 7. "Cooling"), the maximum admissible temperature will be exceeded within a very short time, and the equipment must be switched off. "Emergency" operation at a reduced collector dissipation thus keeps the equipment in service. The following provides a guide for the selection of various operating points at reduced beam current.

The cathode current can be influenced both by the grid No. 1 and grid No. 2 voltages, the interdependence being shown by figs. 29 and 30.

Fig. 31 illustrates the gain G as a function of cathode current I_k at a frequency of 2.6 GHz for reduced cathode current operation. Based on normal operation with $I_k = 85$ mA, $P_o = 20$ W and

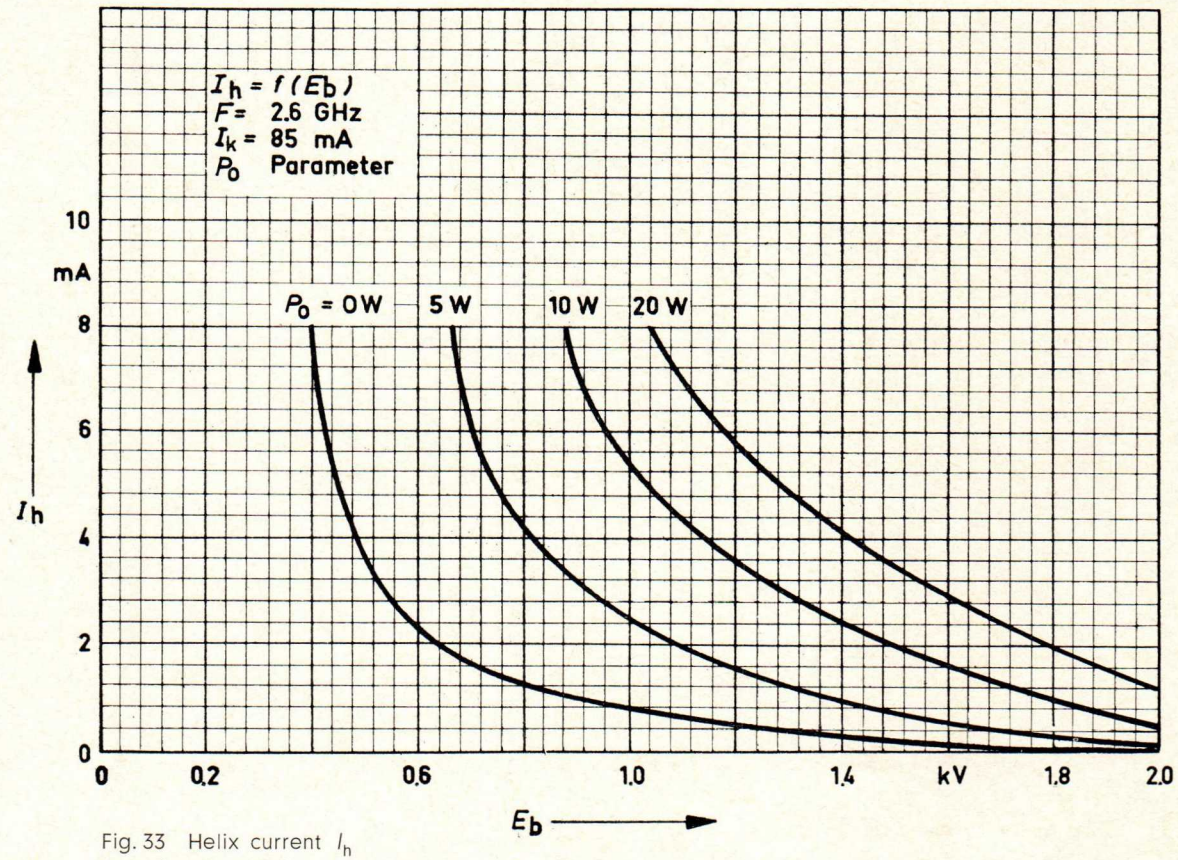

Fig. 33 Helix current I_h
as a function of the collector voltage E_b with the output power P_o as parameter

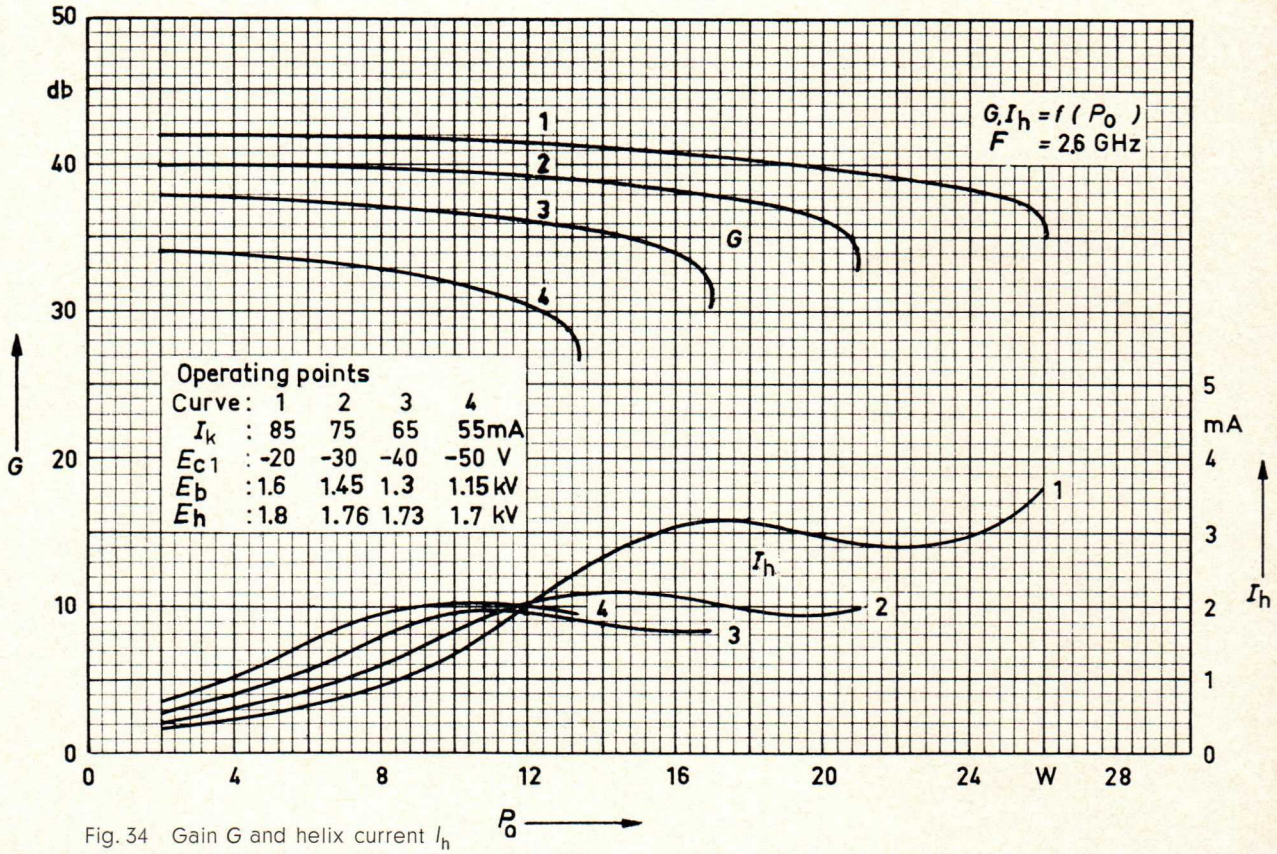

Fig. 34 Gain G and helix current I_h
as functions of the output power P_o for four different operating points

E_h opt = 1.8 kV, the gain with constant input power has been plotted for various cathode currents, first with a constant helix voltage of 1.8 kV, then with optimum helix voltage in each case .Using the curves in fig. 31 of gain with optimized helix voltage, four characteristic operating points for output powers of 20 W, 15 W, 10 W and 5 W at various cathode currents have been selected. For these cathode currents, fig. 34 shows the gain and helix current as functions of the output power

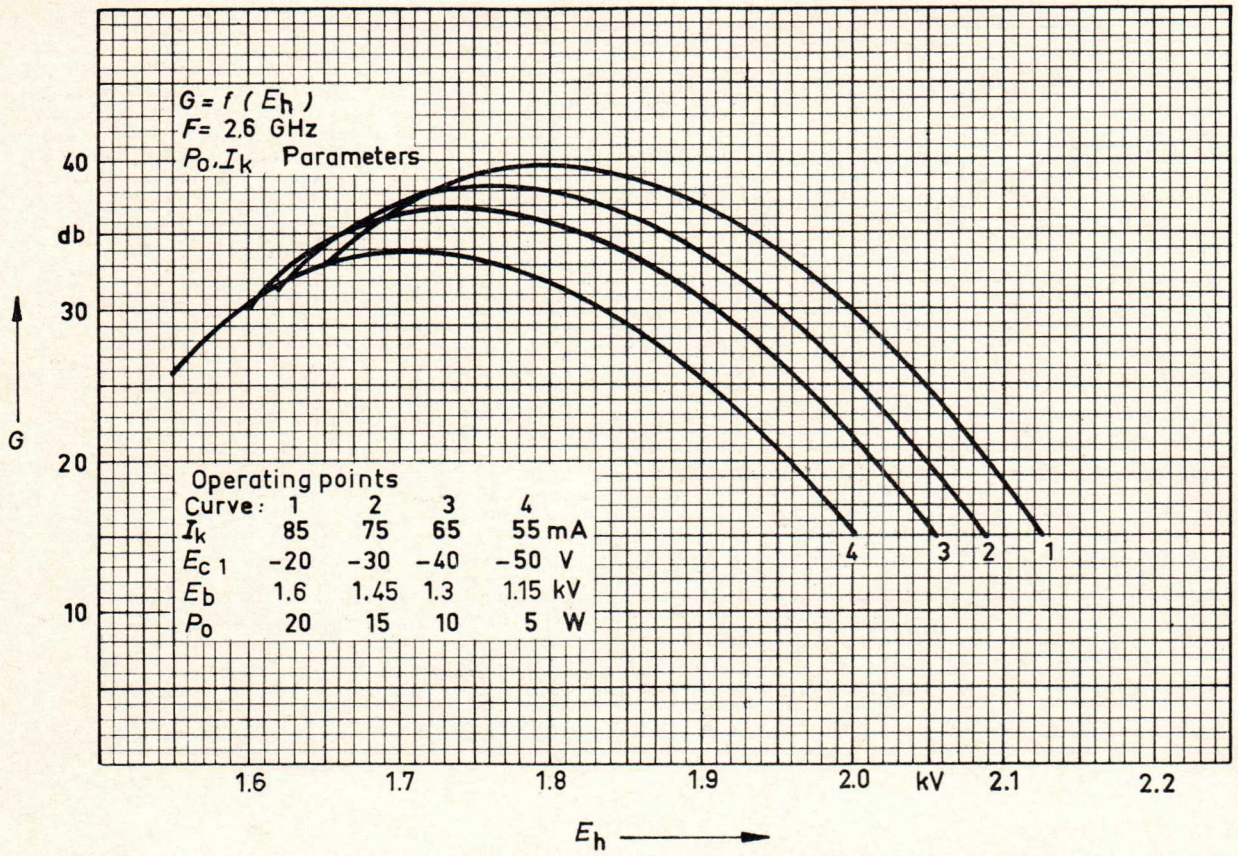

Fig. 35 Gain G as a function of the helix voltage E_h for four different operating points

with constant helix voltage E_h. The associated optimum helix voltage originates from fig. 35. The collector voltage has only been reduced so far that the helix current does not rise above 2 to 3 mA.

In fig. 35 the gain at 2.6 GHz is plotted as a function of the helix voltage, with the four operating points mentioned above (I_k = 85 mA, P_o = 20 W; I_k = 75 mA, P_o = 15 W; I_k = 65 mA, P_o = 10 W; I_k = 55 mA, P_o = 5 W) as parameters.

As the beam current is decreased, the saturation power falls in accordance with the reduced beam energy. Fig. 36 shows the maximum power obtainable P_{sat} dependent on cathode current. The associated optimum helix voltage E_{dl} sat and helix current I_{dl} can also be taken from this diagram. It should be noted that the collector voltage E_b is always reduced with the cathode current I_k. For individual values of cathode current, the collector voltage is given in fig. 36.

The above information is intended for guidance purposes only. Where definite requirements exist for operation at reduced ratings, the manufacturer should be consulted.

5.3. ΔE/PM conversion

Compared with gridded tubes, the electrical length of the interaction space of a traveling-wave tube is very long. The phase velocity of the wave can therefore be influenced by the electron beam, so that variations in the electrode voltages E_{c1}, E_{c2} or E_h produce a phase shift at the output. The ΔE/PM conversion expresses the change in phase angle between input and output voltages per volt change in these electrode voltages. The appropriate values for the RW 21 are:

ΔE_{c1}/PM conversion 1.8°/db
ΔE_{c2}/PM conversion 0.6°/db
ΔE_h /PM conversion 1.5°/db

If the phase modulation is undesired, as is for example the case when the traveling-wave tube is used as a power amplifier in FM microwave radio equipment, the above values can be employed to determine the admissible hum voltage and stability of the power supply.

5.4. Noise

The measure of noise is the noise figure NF, defined as the radio of the signal-to-noise ratio at the output to the signal-to-noise ratio at the input. With it the signal-to-noise ratio at the output of a power tube can be determined easily:

$$\frac{S}{N} = \frac{\text{Signal power}}{\text{Noise power}} = \frac{P_o}{G\ NF\ kT_o\ \Delta F}$$

where

G Gain db
P_o Power output W
kT_o $4 \cdot 10^{-21}$ Ws
ΔF Bandwidth cps
$\frac{S}{N}$ High-frequency energy signal-to-noise ratio
NF Noise figure db

The noise figure of the RW 21 of only 21 db is very low for a tube in this power class.

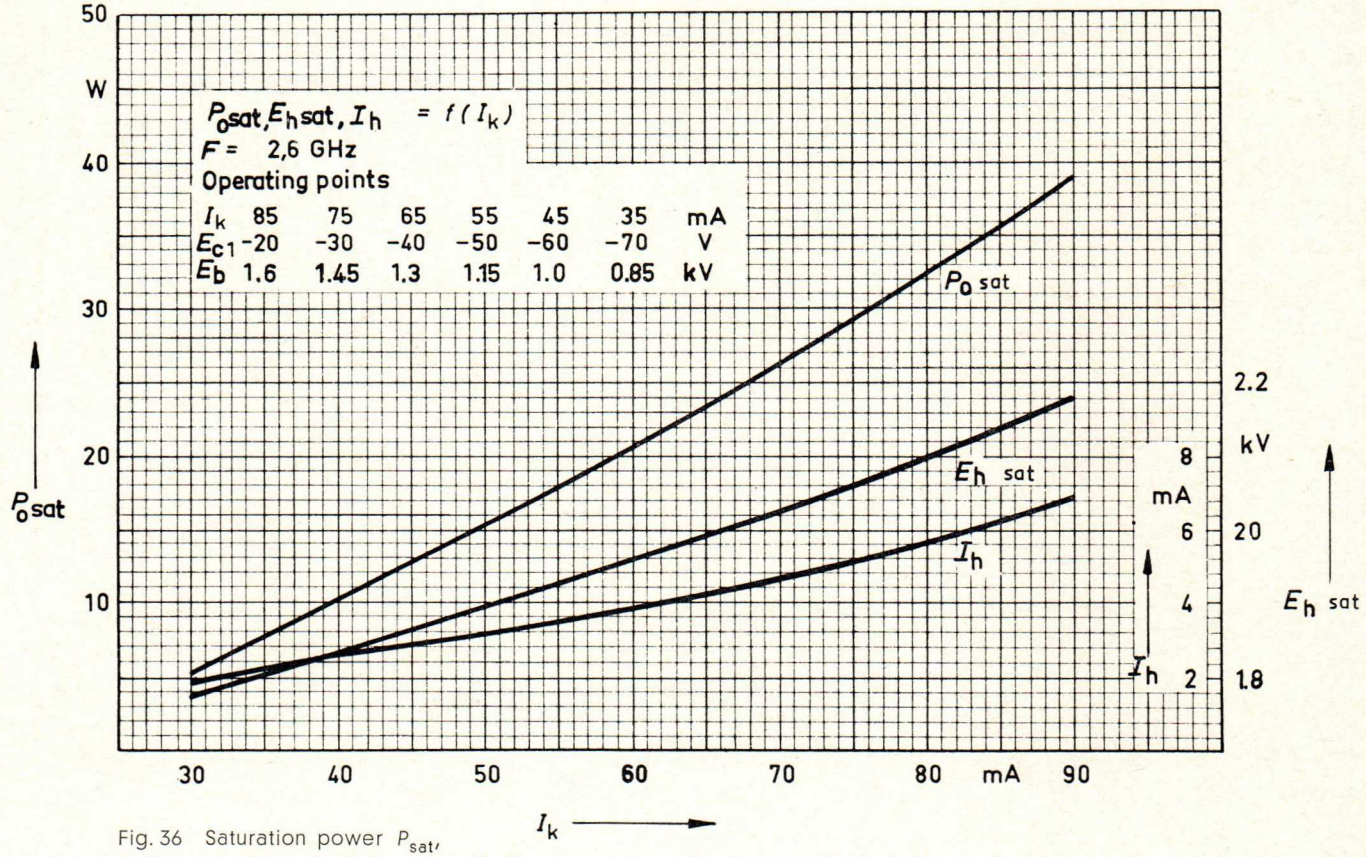

Fig. 36 Saturation power P_{sat}, optimum helix voltage $E_{h\ sat}$ and helix current I_h as functions of the cathode current I_k

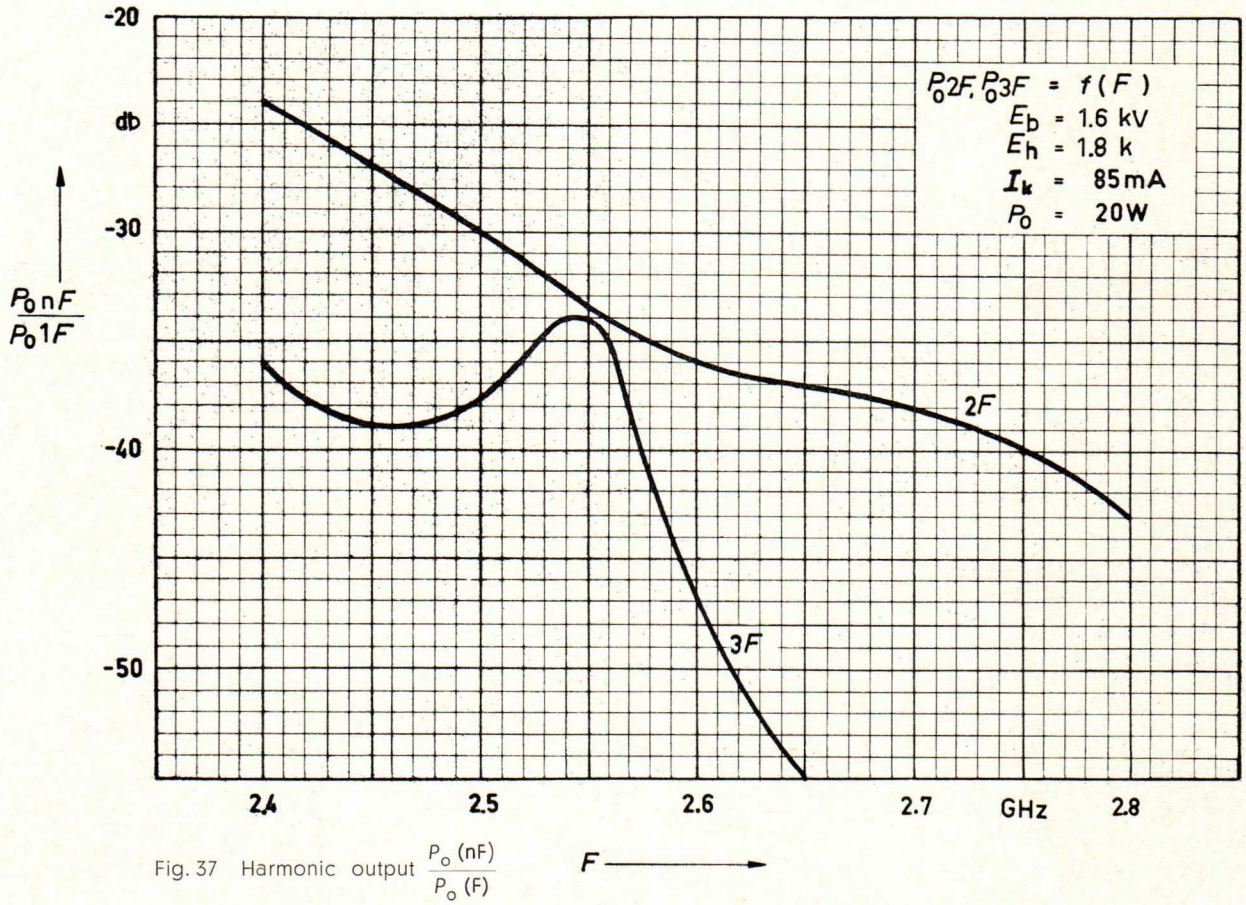

Fig. 37 Harmonic output $\frac{P_o\ (nF)}{P_o\ (F)}$ in decibels as a function of the frequency F for the second and third harmonics

5.5. Harmonic output

As in most active quadripoles, distortion also occurs in the traveling-wave tube which produces harmonics other than the fundamental at the output.

As can be seen from fig. 37, the ratio of harmonic (2F, 3F) to fundamental (F) improves as the frequency increases. In the worst case the second harmonic (2F) at 2.4 GHz is about 24 db down.

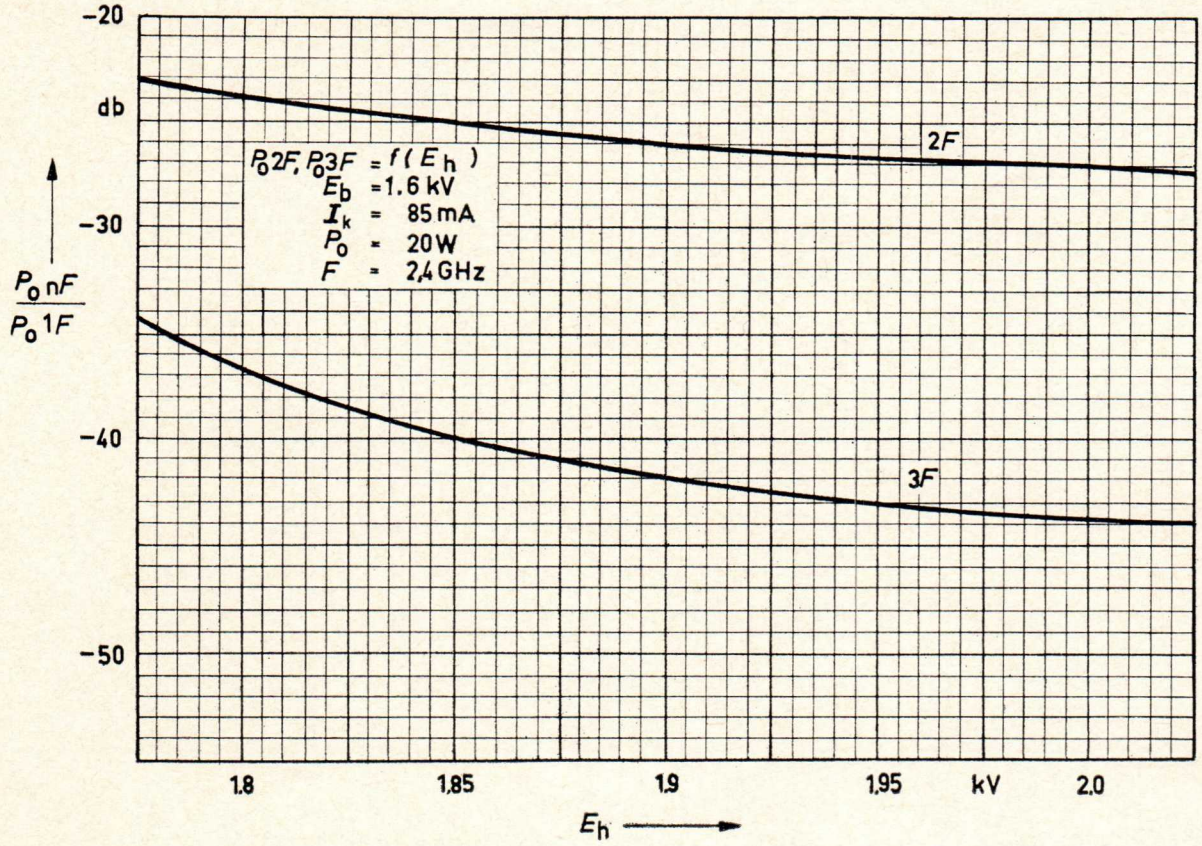

Fig. 38 Harmonic output as a function of the helix voltage E_h for the second and third harmonics

In fig. 38 the effect of helix voltage on harmonic power is plotted at 2.4 GHz. The harmonic content decreases with increasing helix voltage. The optimum helix voltage for an output power of 20 W is approximately 1.8 kV.

5.6. Input and output matching

The large bandwidth of a traveling-wave tube can only be fully exploited if it is possible to make the matching at input and output broadbanded. In practical applications, it is desirable to avoid any individual matching wherever possible, and it is along these lines that the RW 21 has been designed. The RW 21 can be plugged into any magnet system without it being necessary to readjust any matching elements at the output or input, so the tube is a true plug-in match.

The cold input and output VSWR, i. e. without electron beam, is about 1.4:1, and hot the value is less than 1.7:1.

Matching can be further improved by connecting isolators to the input and output, and to utilize the broadband properties to their fullest, this measure is in fact recommended. In doing so, the isolators should be connected as near as possible to the input and output ports to prevent any long-line effects.

5.7. Attenuation

The attenuation of a signal between the output and input of a traveling-wave tube is achieved by depositing a resistive layer on the helix support rods, and this prevents any feedback during operation. It is measured by feeding a certain amount of power into the output and checking the value of the power reaching the input with a super-heterodyne receiver.

The cold attenuation (without electron beam) and hot attenuation (with electron beam) of the RW 21 are both about the same at approximately 80 db. At a gain of 40 db a high safety factor against self-oscillation has thus been provided.

5.8. Short-circuit stability

Normally, traveling-wave tube operate with a well matched load impedance at the normal frequency. Filters between the traveling-wave tube and antenna can, however, cause total reflections with closely adjacent frequencies. Relatively small mismatches in the traveling-wave tube would then lead to self-oscillation due to the high gain.

The traveling-wave tube RW 21 must comply with a stability test in which the input and output of the tube are connected to variable short-circuit lines and the helix voltage swept over a certain range. If the positions of the short-circuit plungers are adjusted independently of each other at random, no self-oscillation or increase in background noise may occur.

6. Operating instructions

The traveling-wave tube RW 21 can only be operated in its magnet system MRW 21.

6.1. Power supplies

Fig. 39 shows the block diagram of a typical traveling-wave tube power supply. The positive terminal of the helix voltage supply unit is grounded.

This means that during normal operation the cathode and heater are floating at a maximum negative potential of 2.2 kV. The heater transformer and

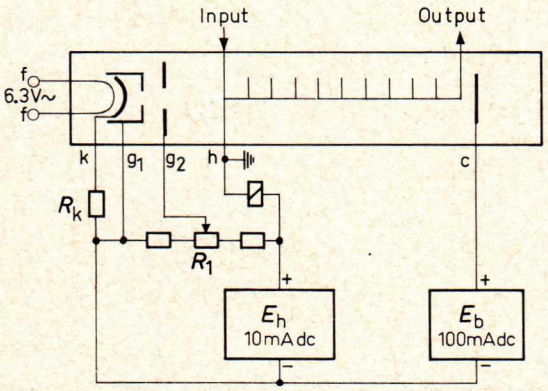

Fig. 39 Block diagram of a power supply

all components at cathode potential must therefore be isolated accordingly. Since the collector voltage is lower than the helix voltage, the collector is negative with respect to the helix, but the following situation must also be taken into consideration: Should the collector voltage of 1.6 kV be applied before the helix and grid No. 2 voltages, initially the collector will rise to 1.6 kV above ground since the helix and cathode are both at the same potential in this instance. Only when the helix voltage of 1.8 kV has been applied will the collector become negative (−200 V) to ground.

When setting the heater voltage to exactly 6.3 V at the tube pins, the voltage drop in the supply cable must be taken into consideration. If the standard cable length of 1.1 m (approx. 43½") is used with the connector socket supplied, the total voltage drop will be 0.1 V.

The grid No. 1 voltage E_{c1} is normally obtained from a voltage drop across the cathode resistor, but a separate source can be employed if desired.

The grid No. 2 voltage E_{c2} should be variable by ± 150 V about the nominal value, and is best derived through a potential divider across the helix voltage supply. The total resistance of the potential divider must not exceed 1 MΩ.

The helix voltage E_h must be variable by ± 250 V about the nominal value. Without considering the current through the potential divider, the helix voltage source must be capable of supplying at least 10 mA. The necessary filtering and stabilization can be determined from information contained in the operating data and curves according to the particular equipment specifications.

Under certain operating conditions, the helix voltage/helix current characteristic of any traveling-wave tube can indicate falling helix current with increasing helix voltage. This means a negative resistance of the helix-to-cathode path. In the interests of stable operation, the helix voltage source should be designed such that its dynamic internal impedance does not exceed the maximum negative helix resistance, which in the case of the RW 21 is about 20 kΩ. This is an absolute maximum value at any frequency. Using present-day power supply techniques, the dynamic internal impedance of the helix voltage source is generally very much lower; values of around 3 kΩ at the resonant frequency of the output filter network, which is the worst case, are quite normal.

The collector voltage E_b requires no special stabilization, but the maximum ratings, in particular the admissible collector dissipation P_p must not be exceeded. The collector voltage source is best designed such that at the nominal mains voltage and desired collector current, the collector voltage is 1.6 kV as specefied in the data. This value may fall by 50 V, or 1.55 kV. Lower values would cause the helix current to rise as demonstrated by figs. 30 and 31. The same principle may also be applied to operation with reduced ratings.

The helix supply lead must contain a current overload relay which automatically switches off the helix and grid No. 2 voltages when the helix current exceeds 10 mA. Switch-on surges of up to 40 Watt-seconds during the first two seconds can be countered by a suitable time constant in the overload relay circuit to prevent the supply from switching off.

If the grid No. 2 voltage is obtained from a separate source it must be interlocked such that when the helix voltage E_h trips out, the grid No. 2 voltage E_{c2} is also removed from the tube simultaneously. When the collector voltage E_b fails, the helix voltage E_{dl} and grid No. 2 voltage E_{c2} must also be switched off either by the overload relay in the helix supply or by a voltage interlock circuit.

6.2. Running-up procedure

6.2.1. Power supply connections

The magnet system must be properly grounded for safety reasons. Before running up the tube, the power supply must be connected to the tube as follows:

a) Collector lead

The high-voltage cable to the collector is connected to the soldering terminal under the removable cover on the cooling assembly.

b) Helix connection

The helix voltage lead is connected to the grounding solder terminal on the magnet system at the coaxial output port.

c) All remaining electrode voltages are applied to the tube through the screened cable with connector socket. The individual leads are color-coded as follows:

Heater	f,f	brown, brown-yellow
Cathode	k	yellow
Grid No. 1	g_1	green, red (should be connected together)
Grid No. 2	g_2	blue
Ground		black

6.2.2. Insertion of the tube into the magnet system

The electron beam can only be correctly guided if the tube is exactly centered in the magnet system. The tube should therefore be cleaned carefully of dirt and metal particles before insertion. It is also advisable to rotate the tube back and forth slightly once it has been inserted, at the same time pressing lightly on the tube base. The following sequence should be adopted:

1) Unscrew the fixing nut and remove the connector socket

2) Slide the tube into the magnet system. The periodic field causes a noticeable counter pressure. If the collector cannot be inserted easily into the cooling fins, the tube should be rotated slightly to overcome the resistance.

3) Rotate the tube such that guide screw on the lug of the magnet system locates in the slot on the side of the tube base.

4) Push on the connector socket and carefully screw the nut on up to the stop. The connector socket should not be tilted otherwise there is a danger of the tube envelope breaking.

6.2.3. Switching the tube on and off

1. Switch-on: either switch on the following simultaneously or in any preferred sequence:

Cooling	
Heater voltage	E_f
Grid No. 1 voltage E_{c1}	(if not derived from the cathode resistance)
Collector voltage	E_b

2. Only if the RW 21 is fired up for the first time or replaced is the preheating time of two minutes required. No preheating is otherwise necessary even for longer interruptions in operation due, for example to mains failures.

3. Next switch on:

Helix voltage E_h Grid No. 2 voltage E_{c2}

either together to the full value (do not run up slowly) or in the sequence helix voltage E_h then grid No. 2 voltage E_{c2}. The condition of simultaneous switch-on is definitely met when the grid No. 2 voltage E_{c2} originates from the potential divider across the helix voltage E_h. It is advisable to set the values of E_{c2} and E_h to those specified on the tube card. Should no card be at hand, E_{c2} is set to about 600 V and E_h to the value specified in the typical operating data.

4. Set the cathode current I_k to the required value by adjusting the grid No. 2 voltage E_{c2}.

5. Adjust for minimum helix current I_h with the aid of the radial field correction (pair of rings, (3) in fig. 7) and axial field correction (single ring, (2) in fig. 7).

6. Apply the high-frequency signal to the input if necessary at a reduced level), and adjust its level alternately with the helix voltage to obtain optimum gain at the desired output power.

7. Carry out the field correction procedure again as in point 5 above.

If for some reason the tube cannot be fired up satisfactorily because the helix current overload relay trips continuously, change the grid No. 1 voltage from −20 V to about −100 V or increase the cathode resistance to several thousand ohms to obtain stronger bunching of the electron beam. The helix current can be minimized with the aid of the correction rings. The grid bias voltage or cathode resistance is then reduced and the prefocusing readjusted again. This procedure should be repeated as often as necessary to bring the values of E_{c1} or R_k back to those specified in the operating data.

The tube can be switched off by removing all electrode voltages simultaneously. If this creates problems, first the beam accelerating voltage E_{c2} (possibly with the helix voltage E_h) should be removed, then the remaining voltages within a short time. **On no account must the collector voltage E_b be switched off before the helix voltage E_h as long as the grid No. 2 voltage is still on,** otherwise the complete beam current will hit the helix. Similarly grid No. 2 would be overloaded if the helix voltage is switched off before the grid No. 2 voltage.

6.3. Safety precautions

The traveling-wave tube RW 21 is operated at high tensions up to 2.2 kV, thus the following points should be observed:

1. The safety regulations applicable to high voltage equipment must be observed.

2. The magnet system and power supply must be properly grounded.

3. The tube may only be replaced when the operating voltages are switched off. For safety reasons it is thus generally necessary to provide some form of automatic voltage cut-out which only permits tube replacement once the voltages are switched off.

6.4. Mounting

The magnet system is magnetically screened and insensitive to external fields. In order to prevent any influence on the beam focusing, the magnet system should still be mounted 50 mm (approx. 2") from ferromagnetic material and 70 mm (approx. 2¾") from external fields. The magnet system should be mounted free of mechanical tension, for example spring metal used to mount the magnet system and flexible coaxial cable connected to the input and output ports. Vibration due to hard shocks and blows must also be avoided. Special dimensional drawings containing all dimensions necessary for mounting are available on request. No alterations to the magnet system and cooling assembly may be carried out.

7. Cooling

The heat developed at the collector can either be removed by convection with an additional air stream or by conduction through some form of good heat-conducting material. Either method of cooling can be used but depends to a certain extent on the actual operating conditions. In normal operation as detailed in section 5.1. under operating data the RW 21 has a collector dissipation of 100 to 140 W, thus natural convection cooling will not suffice.

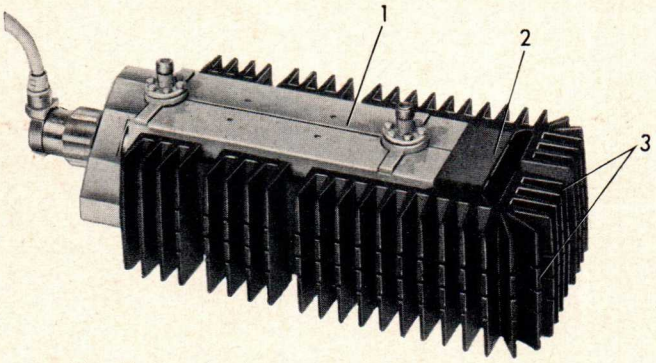

Fig. 40 Conduction-cooled magnet system showing two symmetrically mounted radiators

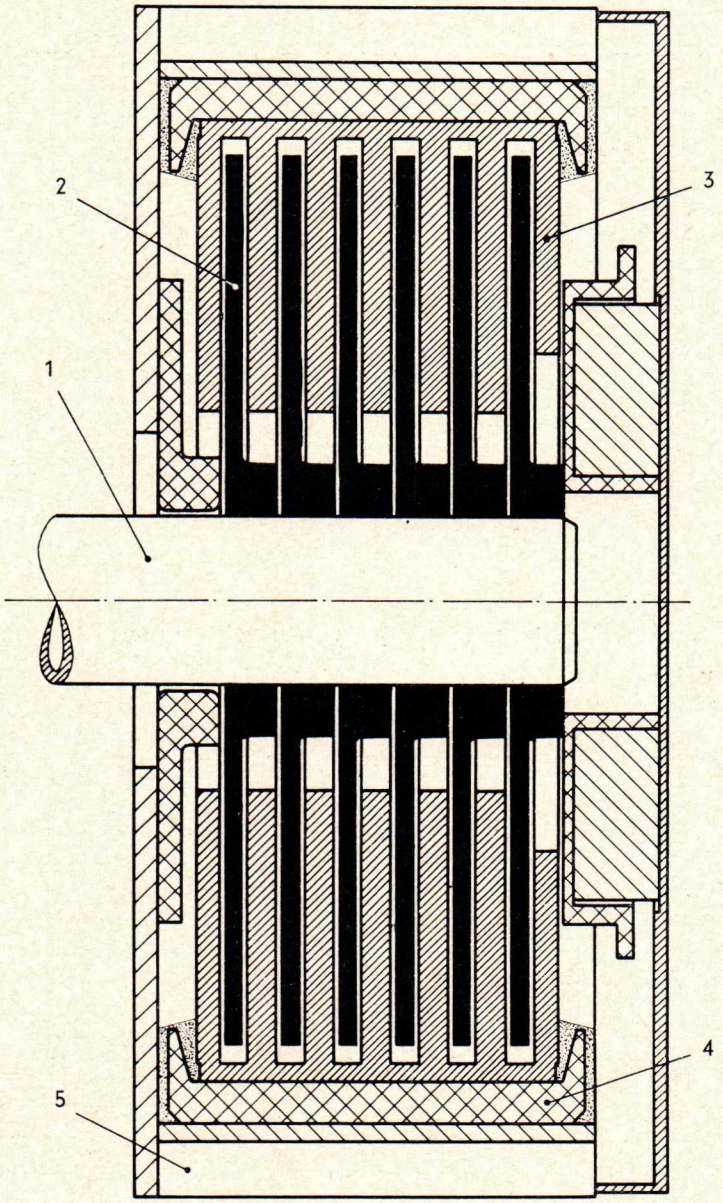

Fig. 41 Sectional drawing of a conduction-cooling assembly for the MRW 21
1 Collector of the RW 21
2 Internal cooling fins
3 Copper comb
4 Insulated copper plate as mounting surface for the external cooling fins

The absolute maximum admissible collector temperature in CW operation of 270 °C governs the method of cooling. In the event of faults the maximum collector temperature may rise to 300 °C for a period of not longer than three days (see also 5.1., footnote 8 under "maximum ratings"). The collector dissipation can be calculated as follows:

$P_p = I_b \, E_b - P_o$

where E_b is the collector voltage, I_b the collector current and P_o the output power.

7.1. Conduction cooling

In the conduction-cooled system the dissipation power in the form of heat is transferred from the collector to two copper plates on the exterior of the magnet system. From these the heat must be dissipated into the surroundings. This can be achieved for example by mounting sets of radiators with a large surface area to the copper plates. Fig. 40 shows such a modified magnet system suitable for natural air cooling.

The conduction-cooling assembly on the magnet system has the same external dimensions as the convection-cooled type, and to a greater extent utilizes the same parts. Fig. 41 illustrates the principle of this assembly.

Two copper combs on opposite sides of the cooling assembly are located between the internal cooling fins. The individual teeth of the comb are slightly thinner than the spacing between the fins, the additional space being required to permit collector insertion into the fins without excessive mechanical resistance. In spite of the air gap the heat transfer is still high because of the large common surface area, and only a small temperature gradient exists across the gaps.

Both copper combs are joined to the two external copper mounting plates through high thermal conductivity insulating discs. Radiators mounted on the

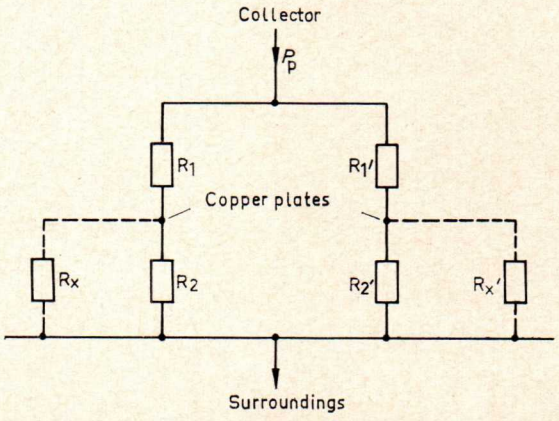

Fig. 42 Equivalent thermal circuit diagram

copper plates can then dissipate the heat into the surroundings. Some form of liquid cooling might also be feasible.

The equivalent thermal circuit diagram for the transfer of heat from the collector to the surroundings has been reproduced in fig 42. The thermal resistances R_1 and R_1' between collector and magnet system are approximately 2.3°/W for the MRW 21a. The dissipation of heat direct from the collector to surroundings is very low and can be safely neglected. The thermal resistance R_2 represents the heat flow through the magnet system and is about 3.2°/W. The values of R_x and R_x' depend on the design of the two radiators, and should be kept as small as possible in the interests of low collector and copper plate temperatures. If the two units are identical, $R_x = R_x'$. The value of R_x also includes the transfer resistance from the copper mounting plate to the radiator, usually about 0.1 to 0.2°/W. The approximate excess temperatures of the collector and copper plates above ambient as functions of the collector dissipation and thermal resistance of the radiator can be obtained from figs. 43 and 44.

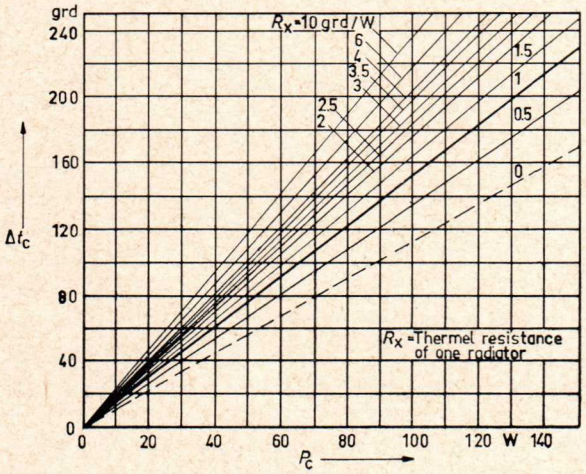

Fig. 43 Excess collector temperature ΔT_c as a function of the collector dissipation P_p for the magnet system MRW 21 with two radiators

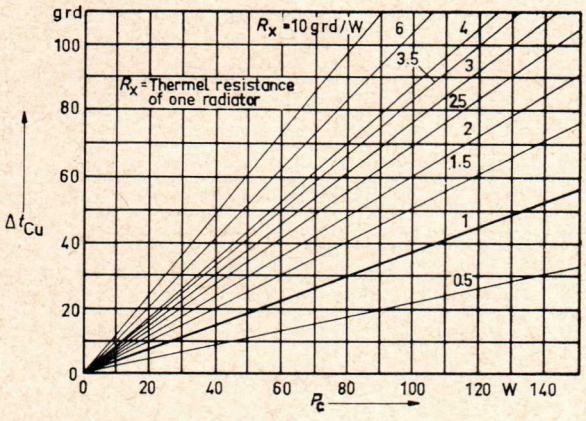

Fig. 44 Excess copper plate temperature ΔT_{cu} as a function of the collector dissipation P_p for the magnet system MRW 21 with two radiators

Design of the radiators

When designing the radiators, it should be taken into consideration that the absolute maximum limits for collector temperature of 270 °C and for copper mounting plates of 115 °C may on no account be exceeded.

The external copper plates on the cooling assembly are electrically isolated from the collector, and are thus at ground potential. When mounting the radiators on the copper plates or magnet system, care should be taken not to exert any mechanical stresses on the plates or that any stresses can occur during operating, otherwise the joints between the ceramic and copper parts could be damaged. For this reason it is recommended that

a) the radiators be slit lengthwise along the axis of the magnet system to compensate for transverse expansion of the copper plates,

b) support the radiator additionally with a mounting bracket on the magnet system to avoid any lever action on the plates,

c) fix the radiators such that inevitable manufacturing tolerances on the radiator and any expansion is considered.

The contact surfaces on the radiators should be plane within 0.02 mm (approx. 1/1000") to guarantee optimum heat transfer.

A radiator suitable for a horizontally-mounted magnet system MRW 21, incorporating the above design aspects, is shown in fig. 45. Such radiators can be supplied as accessories. Similar radiators with cooling fins arranged longitudinally for vertically-mounted magnet systems are also available. The thermal resistance of these radiators is about 1°/W. The appropriate lines on the graphs in figs. 43 and 44 are shown thicker.

The magnet system should not be carried by the radiators, and when the magnet system is shipped outside the equipment, the radiators must be dispatched separately.

7.2. Convection cooling

The exterior of the convection-cooling assembly is shown in fig. 21. This assembly contains six pairs of cooling fins which are spring loaded on the collector (sectional drawing see fig. 41 „cooling fins"). The edges of the cooling fins are located in two ceramic supports which insulate them from the housing.

A magnet system fitted with a convection-cooling assembly can either be natural of forced-air cooled. At normal operating conditions the air flow rate must be at least 5.3 cu ft/min (150 l/min). The relationship between collector temperature T_c' collector dissipation P_p and quantity of air V can be taken from fig. 46. With time the circulation of air through the cooler can produce fouling-up of the internal cooling fins with dust and possibly other foreign matter, which in turn decreases the efficiency of the cooling system. When using any form of blower, it is therefore advisable to filter the air before it is blown across the cooling fins and also to clean or replace the filters at suitable intervals. It should be noted that the absolute col-

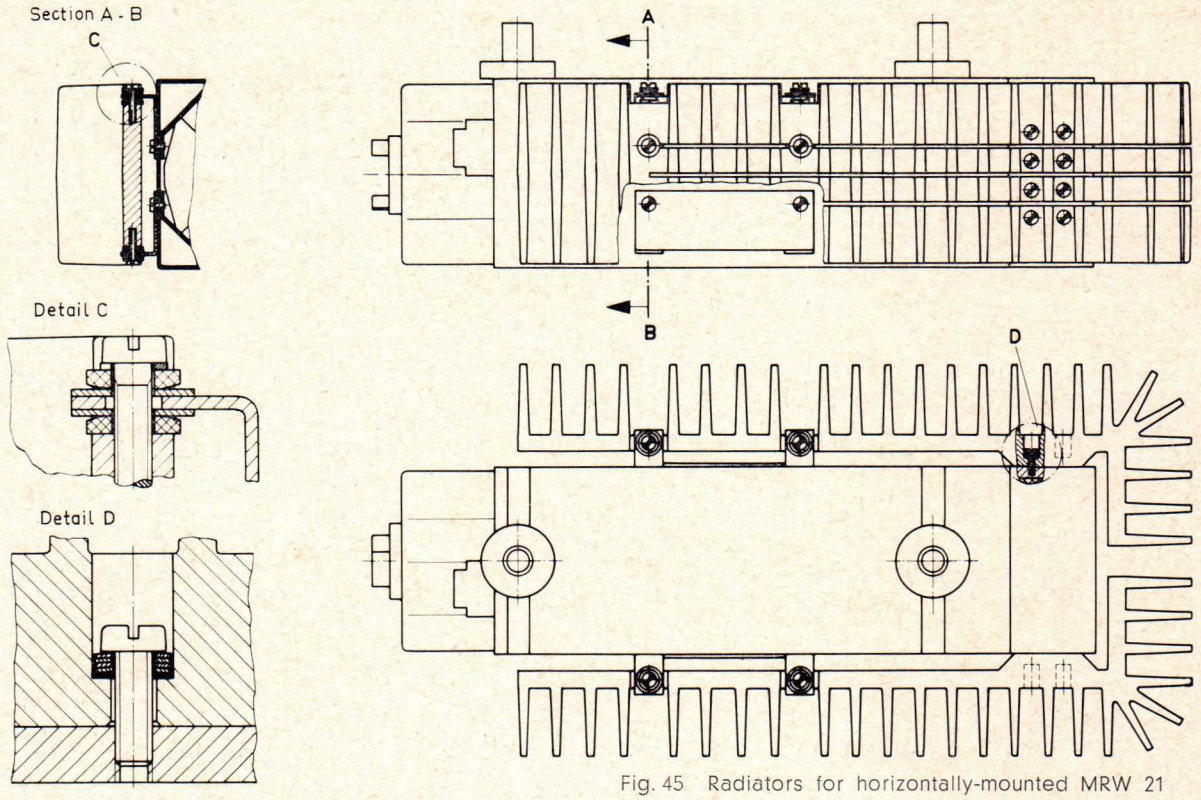

Fig. 45 Radiators for horizontally-mounted MRW 21

lector temperature T_c is equal to the excess collector temperature ΔT_c plus ambient temperature T_A.

For a collector dissipation of up to 55 W ("emergency operation") no special cooling is required, provided the magnet system is mounted horizontally and natural air circulation through the cooler housing can be guaranteed. In this case the ambient temperature may not exceed 50 °C. A natural air circulation of this nature corresponds to about 0.3 cu ft/min (8 to 10 l/min). If the cooler is rather unfavorably positioned, e. g. the opening on one side is covered, the cooling fins are no longer effective, and the heat will be conducted away to

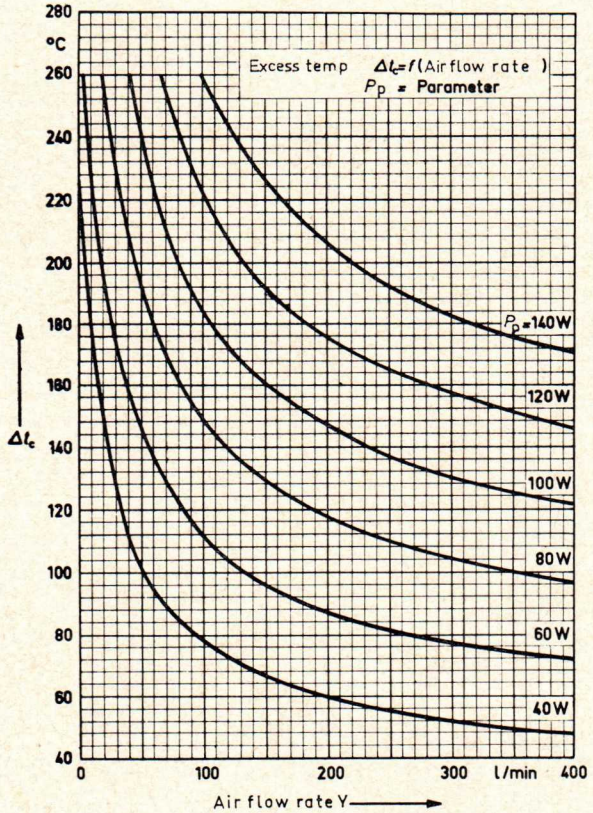

Fig. 46 Excess collector temperature ΔT_c as a function of the necessary amount of cooling air V with the collector dissipation P_p as parameter

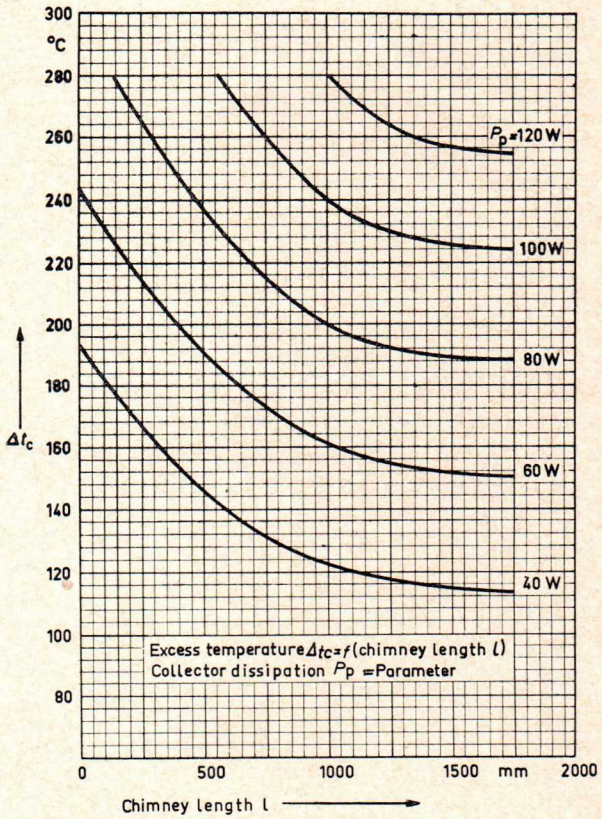

Fig. 47 Excess collector temperature ΔT_c as a function of the chimney length l with the collector dissipation P_p as parameter

		Normal operation with blower	Operation at reduced ratings when the blower fails		
			with 1 m chimney	without chimney	
Collector voltage	E_b	1.5	1.2	1.0	kV
Cathode current	I_k	90	80	55	mA
Gain, approx.	G	41	39.5	34	db
Sync power	P_{syn}	10	7	2	W
Collector dissipation, approx.	P_p	135	95	55	W
Excess collector temperature approx.	ΔT_c	185	230	220	°C
Air flow rate	V	10	2	0.3	cu ft/min

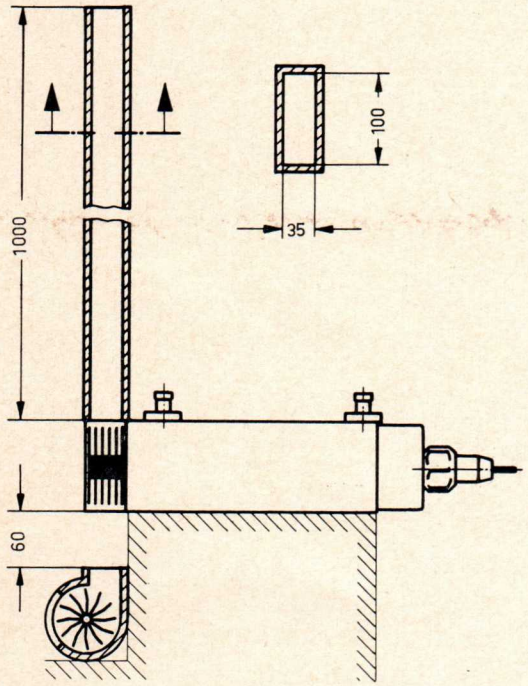

Fig. 48 The magnet system RW 21 with convection-cooling assembly blower and chimney combined

the outer surface of the housing and radiated into the surroundings. The excess temperature will thus be higher. The values for 0 cu ft/min can be obtained from fig. 46.

Cooling can be improved considerably by a chimney of the same cross section as the sides of the cooling assembly mounted vertically above the cooler. Fig. 47 gives the required chimney height for various dissipation powers, whereby chimney lengths above 1 m do not produce much further improvement in cooling. The curves are based on a chimney cross section of about $1^3/_8$" × 4" (35 mm × 100 mm). Using this method of cooling the air must be able to flow unhindered into the lower opening of the cooler. The chimney should be made from thermal insulating material so that the air cannot cool off and thereby reduce the suction effect.

A combined arrangement of blower and chimney is shown in fig. 48, with which it is possible to operate the tube at a relatively high power under "emergency" conditions should the blower fail.

For tv operation with concurrent video and audio transmission, the following table indicates the power obtainable and the admissible operating data with three different states of cooling.

It can be seen that using a chimney when the blower fails means the output power need only be reduced to 70 %, whereas without a chimney it must be dropped to 20 % of the nominal value.

The values of excess collector temperature and air flow rate are based on the arrangement shown in fig. 48. In principle, continuous operation of the RW 21 with reduced cathode current and collector voltage is also permissible provided the absolute maximum collector temperature of 270 °C is not exceeded.

8. Coaxial accessories

8.1. Coaxial rf connectors

The magnet system MRW 21 can be supplied with the following coaxial ports

50 Ω coaxial ports $^{3}/_{7}$ (N connector) or $^{7}/_{16}$
60 Ω coaxial ports 3.5/9.5 or $^{6}/_{16}$

8.2. Isolators

It is advisable to use isolators at the input and output of the travling-wave tube; both protect the tube against load faults, and suppress reflections and thus prevent additional channel noise. These isolators should be connected as near as possible to the input and output ports to avoid any long-line effects (see section 5.6. "Matching").

8.3. Harmonic filters

Harmonics at the output due to non-linearity in the tube characteristics can be suppressed by low-pass or band-pass filters (see section 5.5. "Harmonic output").

9. Ordering specifications

When ordering the RW 21, magnet system MRW 21 and connector sockets the ordering numbers quoted below should be specified. The various arrangements available have been sumarized in fig. 49.

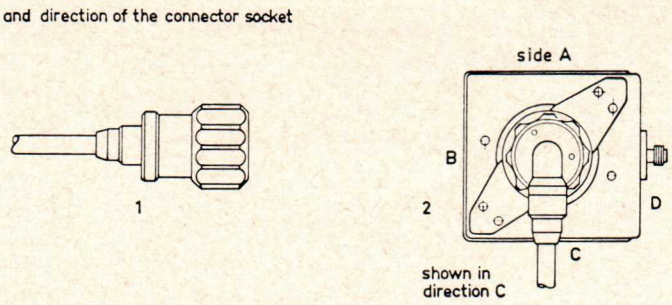

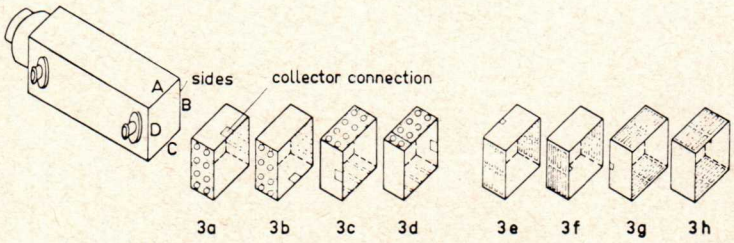

Fig. 49 1 Straight connector socket
2 Connector socket with 90° bend in direktion C
3a to 3h Various arrangements of mounted cooling assembly and collector connection

9.1. Ordering numbers for traveling wave tube RW 21 and connector sockets

Designation	Design		Ordering numbers
Traveling-wave tube RW 21			Q00041-X3256
Connector socket	axial	standard cable length 1.2 m (1)	Q00081-X2321
Connector socket	bend in direction A		Q00081-X2322
Connector socket	bend in direction B		Q00081-X2323
Connector socket	bend in direction C		Q00081-X2324
Connector socket	bend in direction D		Q00081-X2325
Connector socket	axial	cable length as required (2)	Q00081-X2315
Connector socket	bend in direction A		Q00081-X2316
Connector socket	bend in direction B		Q00081-X2317
Connector socket	bend in direction C		Q00081-X2218
Connector socket	bend in direction D		Q00081-X2319

(1) 0.1 m of this length as free leads.
(2) When ordering please specify total length of cable and length of free leads.

9.2. Ordering numbers for magnet systems MRW 21

Designation	Design			Ordering numbers Q00043-X . . .			
	Cooling	Cooling in direct.	Collect connect. at side	Coaxial connections 3.5/9.5	3/7(1)	7/16	6/16
Magn.syst. MRW 21a11	Conduction	B-D	A	2441	2451	2461	2471
Magn.syst. MRW 21a12		B-D	C	2445	2455	2465	2475
Magn.syst. MRW 21a21		A-C	D	2442	2452	2462	2472
Magn.syst. MRW 21a22		A-C	B	2446	2456	2466	2476
Magn.syst. MRW 21b11	Convection	B-D	A	2443	2453	2463	2473
Magn.syst. MRW 21b12		B-D	C	2447	2457	2467	2477
Magn.syst. MRW 21b21		A-C	D	2444	2454	2464	2474
Magn.syst. MRW 21b22		A-C	B	2448	2458	2468	2478

(1) N-connector

9.3. Typical ordering specification

The ordering numbers for traveling-wave tube, magnet system and connector socket with cable should be stated separately.

For example:

Traveling-wave tube RW 21	Q 00041 - X3256
Magnet System MRW 21b12, convection cooling direction B-D collector connection side C	
coaxial ports $^{7}/_{16}$ (50 Ω)	Q 00043 - X2467
and connector socket with bend in direction D	Q 00081 - X2319/2 m long
cable 2 m, 0.1 m free ends	0.1 m free ends

10. References

[1] W. Eichin and G. Landauer. Beeinflussung von Gewinn und Stabilität einer Wanderfeldröhre durch Wahl des Flächenwiderstandes ihrer Dämpfungsschicht.
NTZ No. 11 (1958) Issue 3 pp 131 to 137.

[2] P. Meyerer, Permanentmagnetische Fokussierungsanordnungen für Höchstfrequenzröhren. AEÜ No. 15 (1961) Issue10 pp 467 to 474.

SIEMENS

From the Siemens Product Range

Traveling Wave Tubes
for radio link systems and TV transmitters
from 0.5 to 8.5 GHz and 5W to 3kW

Backward Wave Oscillators
voltage tunable
from 26.5 to 90 GHz

Resonant Backward Wave Oscillators
mechanical and voltage
tunable from
6.5 to 12.7 GHz and 32.5 to 40 GHz

Reflex Klystrons
as linear modulators from 3.6 to 6.0 GHz

Planar Triodes and Tetrodes
in metal-ceramic up to 7 GHz

Power Tubes
radiation, air, water and vapor cooled
glass and ceramic types
for transmitters and industrial heating

High-Voltage Rectifiers

Thyratrons

Special Purpose Tubes
comprehensive range
for professional applications
long life and high reliability

Stabilizers Tubes

Numeric and symbolic indicator tubes

Cathode ray tubes

Vidicons

Gas Lasers

Voltage surge protectors

Receiving and TV Picture Tubes

Selenium and Silicon Rectifiers

Selenium stabilizers

Bestell-Nr. 2-6220-015-01 Printed in Germany

10661.5